

CALET

Calorimetric
Electron
Telescope



Pier Simone Marrocchesi

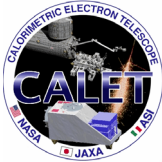
University of Siena & INFN-Pisa

for the CALET Collaboration

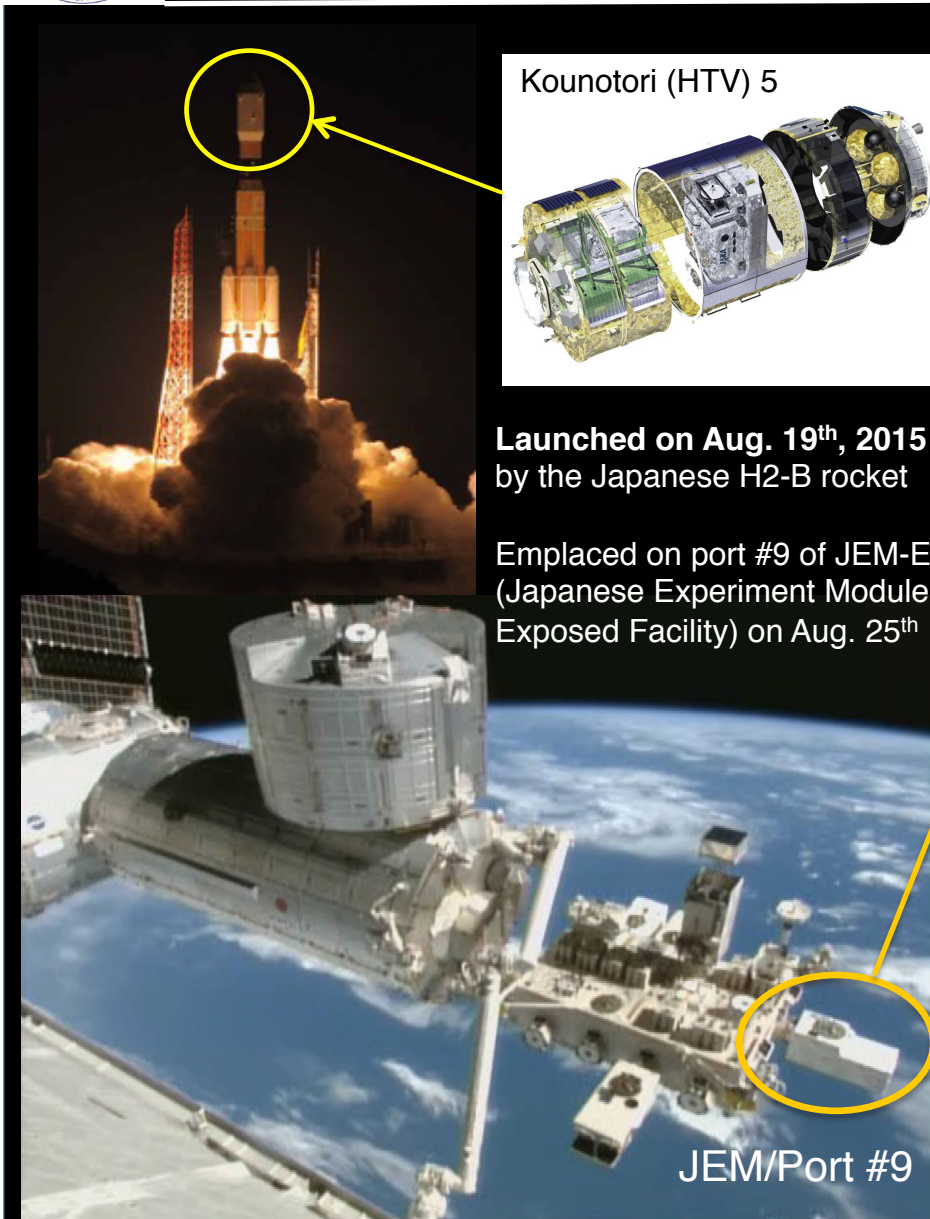
XSCRC - 2019

CERN, 2019 Nov 13-15

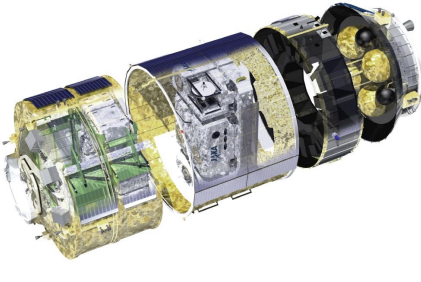




CALET Payload



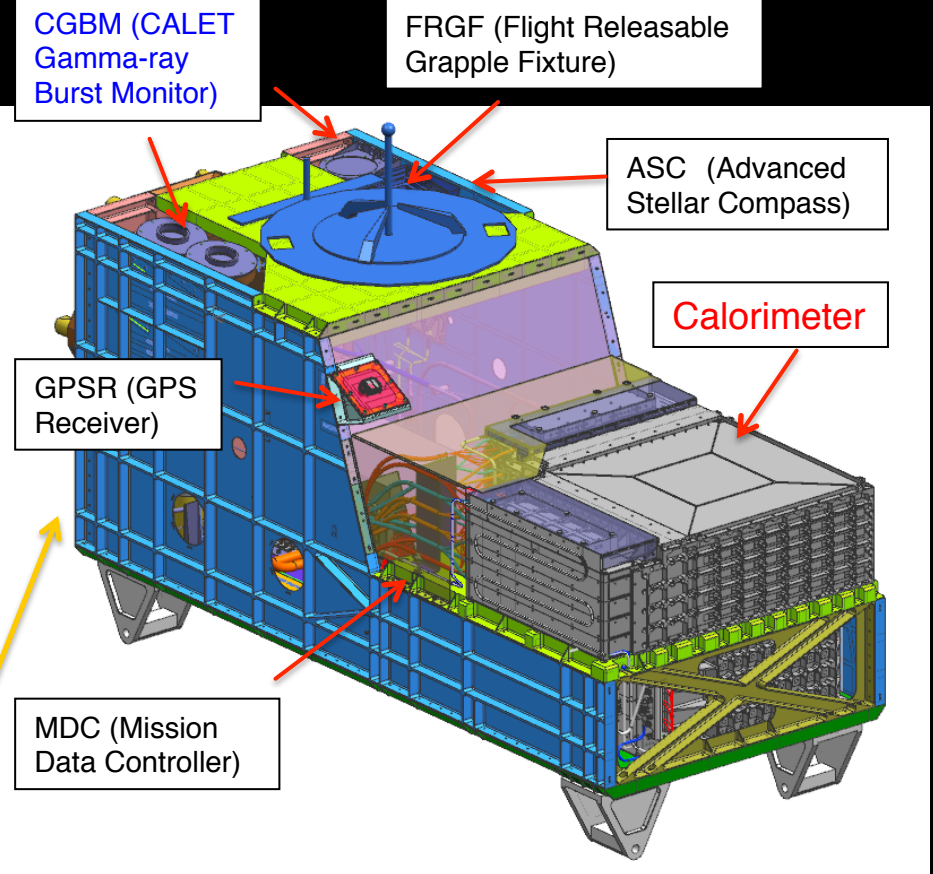
Kounotori (HTV) 5



Launched on Aug. 19th, 2015 by the Japanese H2-B rocket

Emplaced on port #9 of JEM-EF (Japanese Experiment Module Exposed Facility) on Aug. 25th

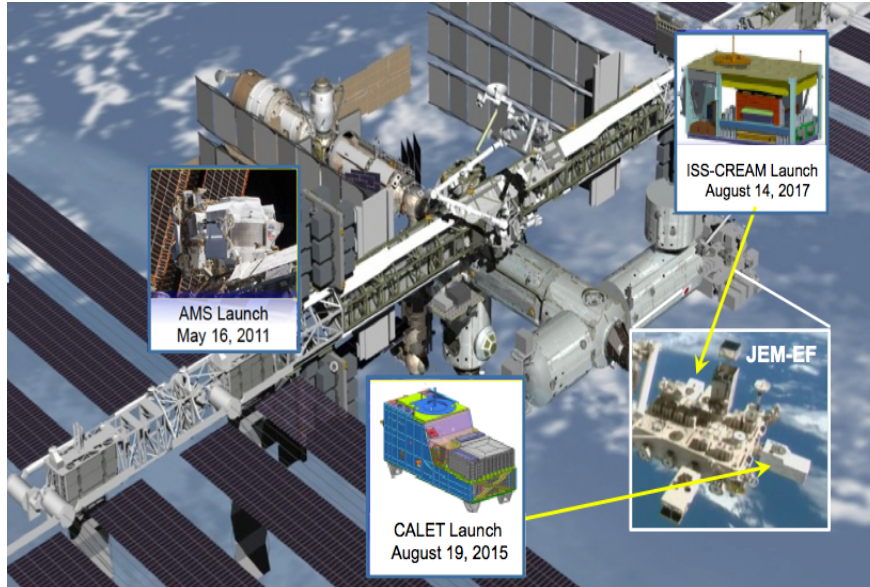
JEM/Port #9



- **Mass:** 612.8 kg JEM Standard Payload
- **Size:** 1850mm (L) × 800mm (W) × 1000mm (H)
- **Power:** 507 W (max)
- **Telemetry:** Medium 600 kbps (6.5GB/day)



Cosmic Ray Observations aboard the ISS and CALET program



Main CALET science objectives:

- ✧ **Electron observation** in 1 GeV - 20 TeV range. Design optimized for electron detection: high energy resolution and large e/p separation power + e.m. shower containment. Detailed study of spectral shape. **Search for Dark Matter and Nearby Sources**
- ✧ **Observation of cosmic-ray nuclei** in the energy region from 10 GeV to 1 PeV. **Unravelling the CR acceleration and propagation mechanism(s)**
- ✧ Detection of **transient phenomena** in space **Gamma-ray bursts, e.m. GW counterparts, Solar flares, Space Weather**

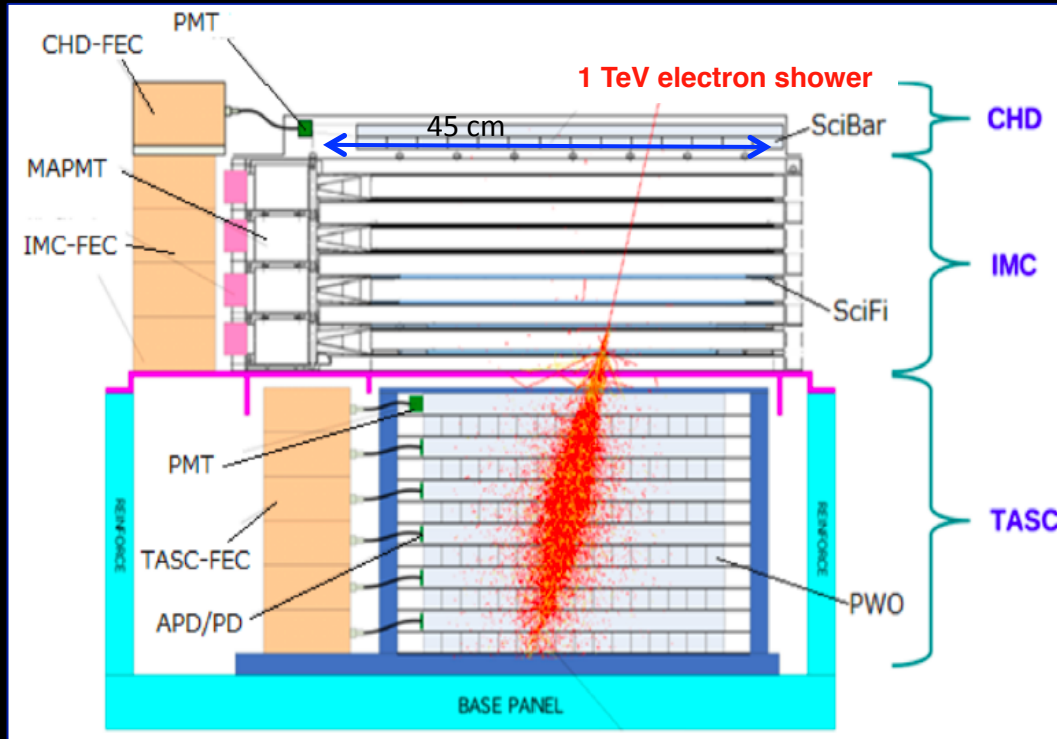
Scientific Objectives	Observation Targets	Energy Range
CR Origin and Acceleration	Electron spectrum Individual spectra of elements from proton to Fe Ultra Heavy Ions ($26 < Z \leq 40$) Gamma-rays (Diffuse + Point sources)	1 GeV - 20 TeV 10 GeV - 1000 TeV > 600 MeV/n 1 GeV - 1 TeV
Galactic CR Propagation	B/C and sub-Fe/Fe ratios	Up to some TeV/n
Nearby CR Sources	Electron spectrum	100 GeV - 20 TeV
Dark Matter	Signatures in electron/gamma-ray spectra	100 GeV - 20 TeV
Solar Physics	Electron flux (1 GeV-10 GeV)	< 10 GeV
Gamma-ray Transients	Gamma-rays and X-rays	7 keV - 20 MeV



CALET instrument in a nutshell

Field of view: ~ 45 degrees (from the zenith)

Geometrical Factor: $\sim 1,040 \text{ cm}^2\text{sr}$ (for electrons)

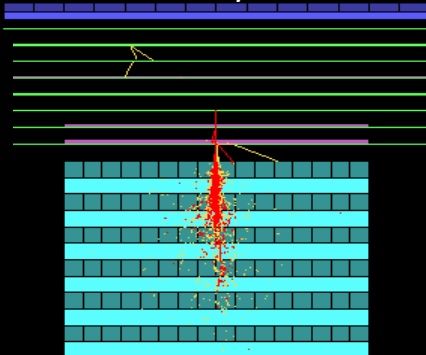


CALET: a unique set of key instruments

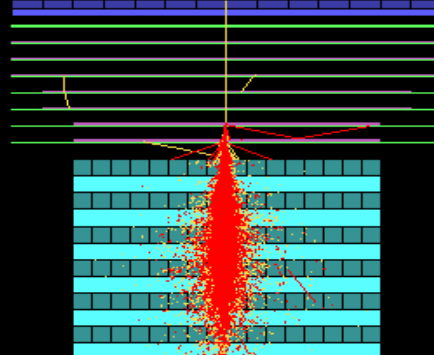
- **CHD**: a dedicated **charge detector + multiple dE/dx sampling in the IMC** allow the **identification of individual nuclear species** (charge resolution $\sim 0.15\text{-}0.3 e$).
- **IMC**: **high granularity (1mm) imaging pre-shower calorimeter** to accurately reconstruct the **arrival direction** of incident particles ($\sim 0.1^\circ$) and the **starting point** of electro-magnetic showers.
 SciFi + Tungsten absorbers: $3 X_0$ ($= 0.2 X_0 \times 5 + 1.0 X_0 \times 2$)
- **TASC**: thick ($27 X_0$) homogeneous PWO calorimeter allowing to extend electron measurements into the TeV energy region with $\sim 2\%$ **energy resolution**.
- **Combined** ($30 X_0, 1.2 \lambda_1$) they **separate electrons** from the abundant protons (rejection $> 10^5$).

Simulated Shower Profile

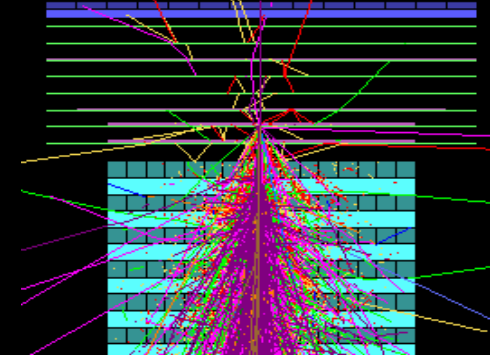
Gamma-ray 10 GeV



Electron 1 TeV

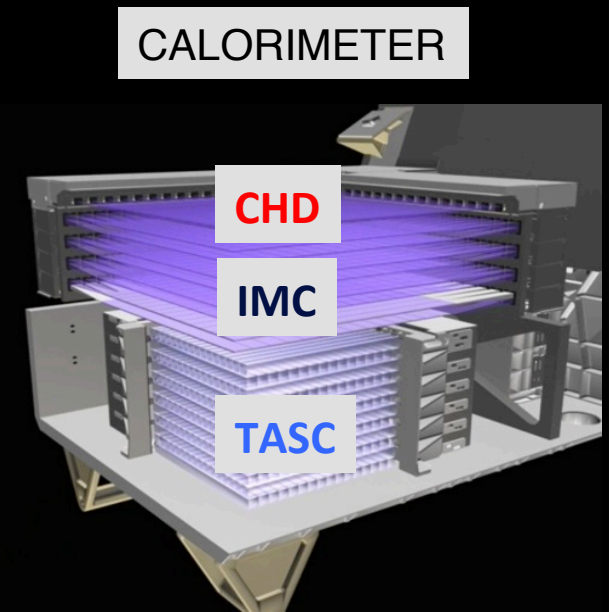
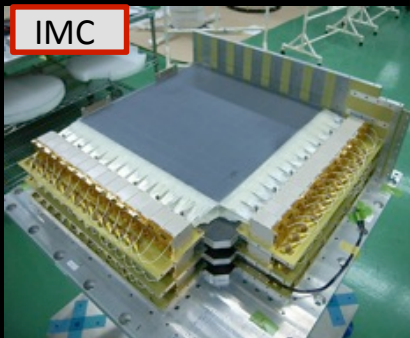
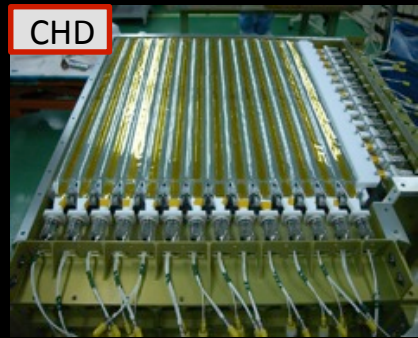


Proton 10 TeV





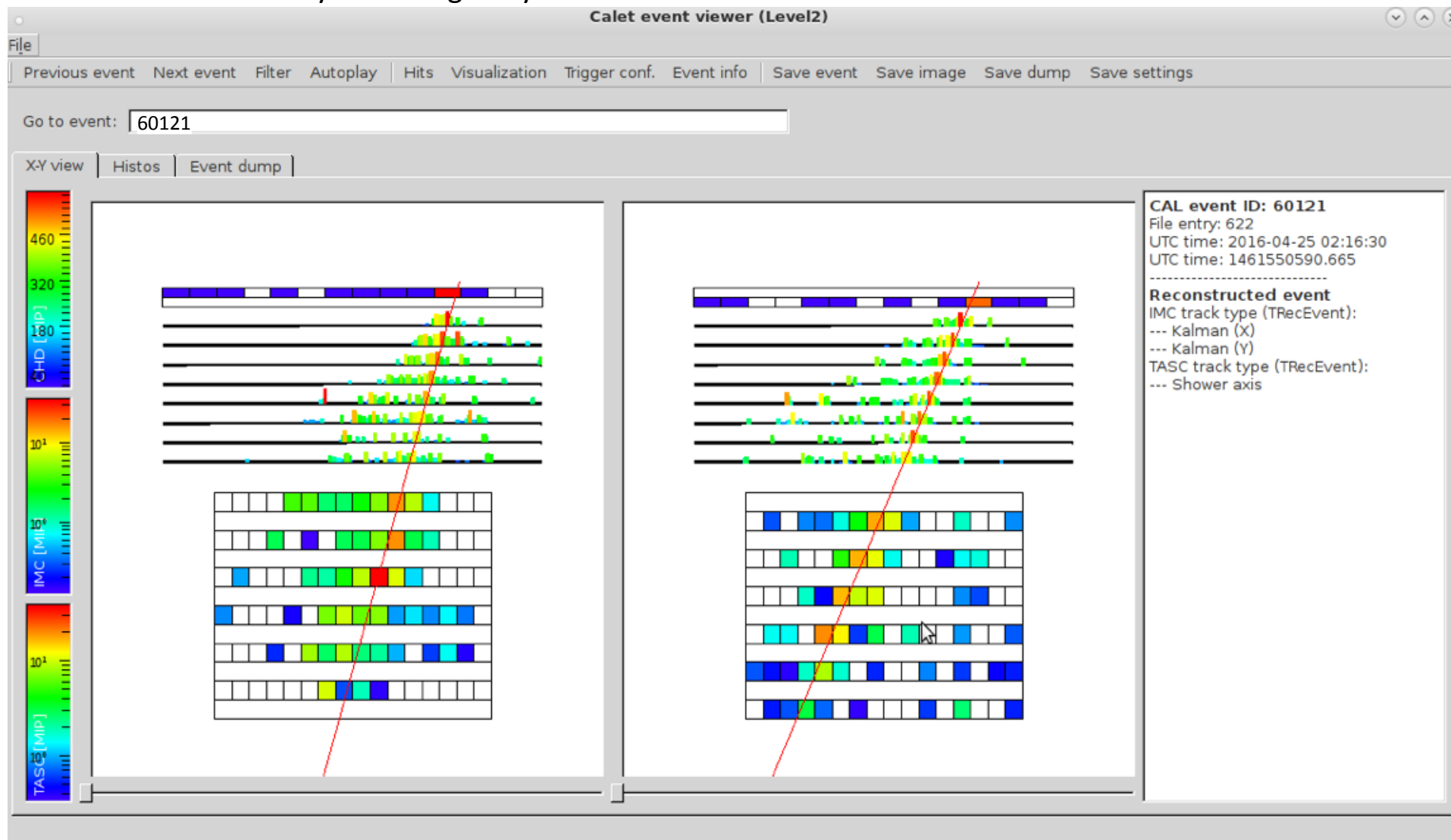
CALET Instrument overview



	CHD (Charge Detector)	IMC (Imaging Calorimeter)	TASC (Total Absorption Calorimeter)
Measure	Charge (Z=1-40)	Tracking , Particle ID	Energy, e/p Separation
Geometry (Material)	Plastic Scintillators: 28 paddles 14 paddles x 2 layers (X,Y) Paddle Size: 32 x 10 x 450 mm ³	Scintillating Fibers: 448 x 16 layers (X,Y) Scifi size: 1 x 1 x 448 mm ³ 7 Tungsten layers : 0.2X ₀ x 5 + 1X ₀ x 2 Total Thickness: 3 X ₀	PWO logs: 16 x 12 layers (x,y): 192 logs log size: 19 x 20 x 326 mm ³ Total Thickness: 27 X ₀ , ~1.2 λ _i
Readout	PMT+CSA	64-anode PMT+ ASIC	APD/PD+CSA PMT+CSA (for Triggerer)@top layer

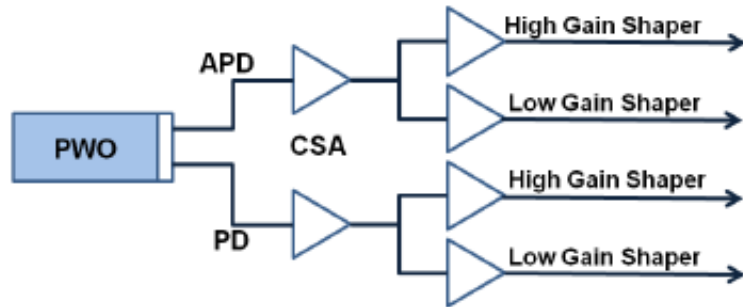
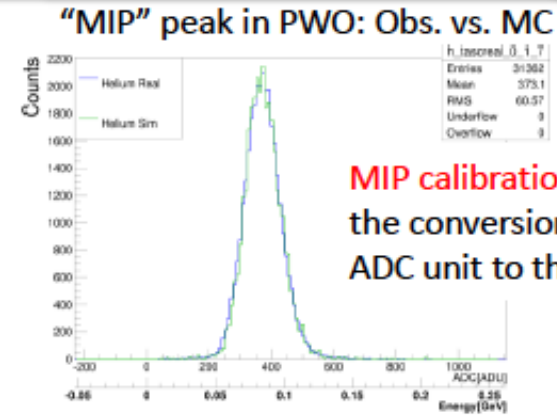
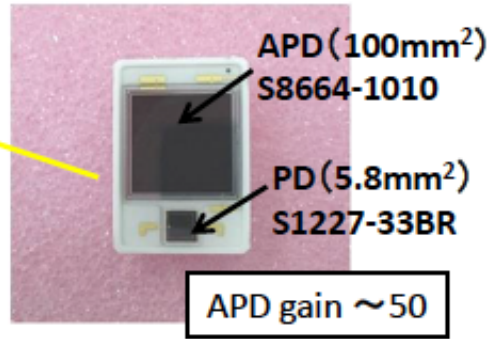
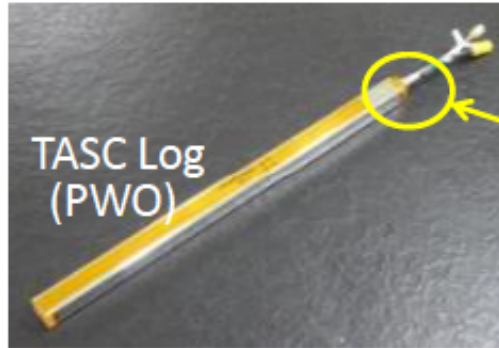
✧ CALET **tracking** takes advantage of the IMAGING capabilities of IMC thanks to its granularity of **1 mm with Sci-fibers readout individually**

Example: A **multi-prong event** due to an interaction of the primary particle in the CHD is very well imaged by the IMC.





Energy Measurement in a wide dynamic range 1-10⁶ MIPs

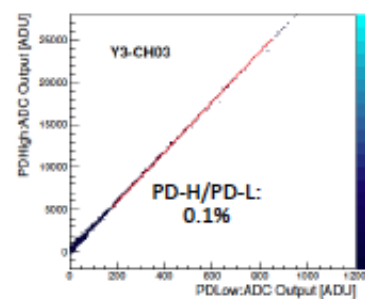
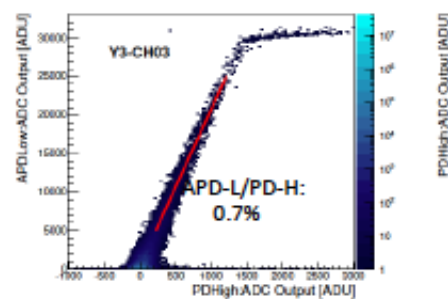
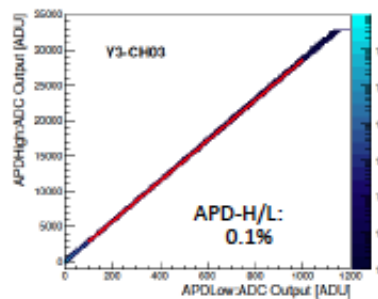


The whole dynamic range was calibrated by **UV laser irradiation** on ground :
 1) The linearity of each gain range is confirmed in the range of 1.4-2.5 %.
 2) Each channel covers from 1 MIP to 10⁶ MIPs.

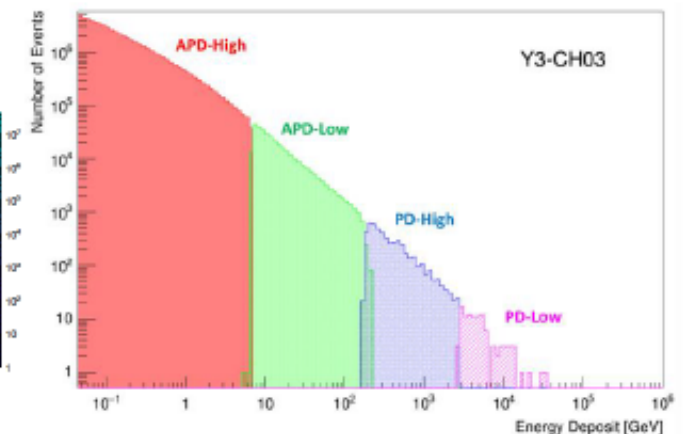
APD-H	APD-L	PD-H	PD-L
1.4%	1.5%	2.5%	2.2%

The correlation between adjacent gain ranges is calibrated by using **in-flight data** in each channel.

APD-H APD-L	APD-L PD-H	PD-H PD-L
0.1%	0.7%	0.1%



Example of energy distribution in one PWO log





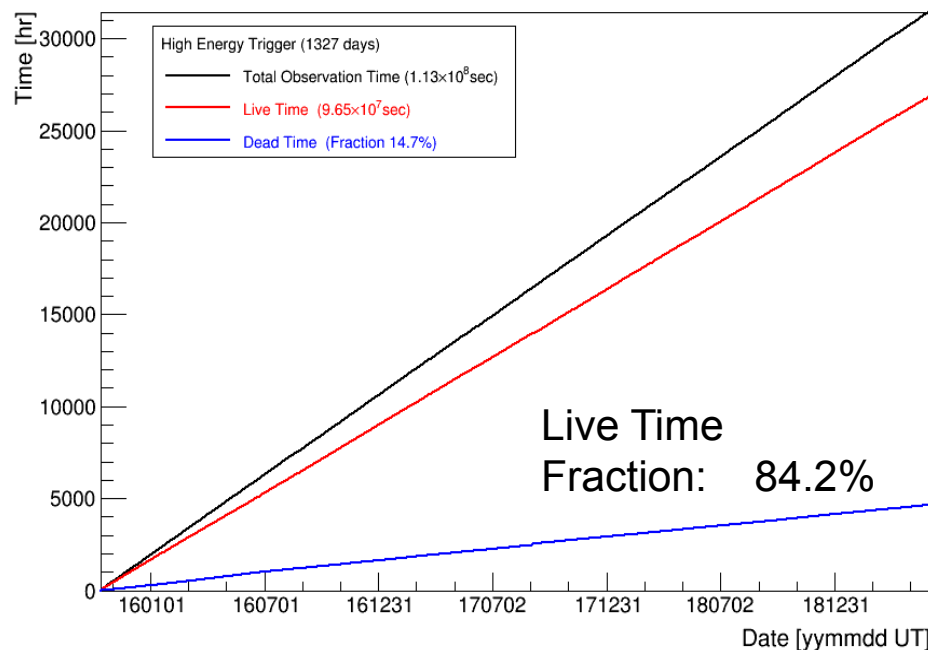
Observations with High Energy Trigger (>10GeV)

Observation with High Energy Trigger for 1327 days : Oct.13, 2015 – May 31, 2019

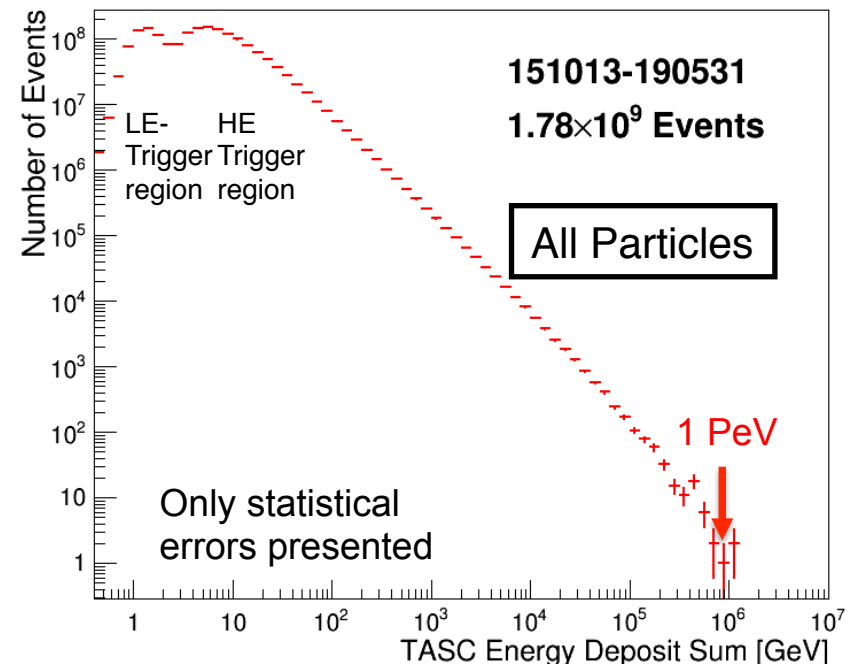
□ The exposure, SQT , has reached $\sim 116 \text{ m}^2 \text{ sr day}$ for electron observations under continuous and stable operations.

□ Total number of triggered events is $\sim 1.8 \text{ billion}$ with a live time fraction of $\sim 84 \%$.

Accumulated observation time (live, dead)



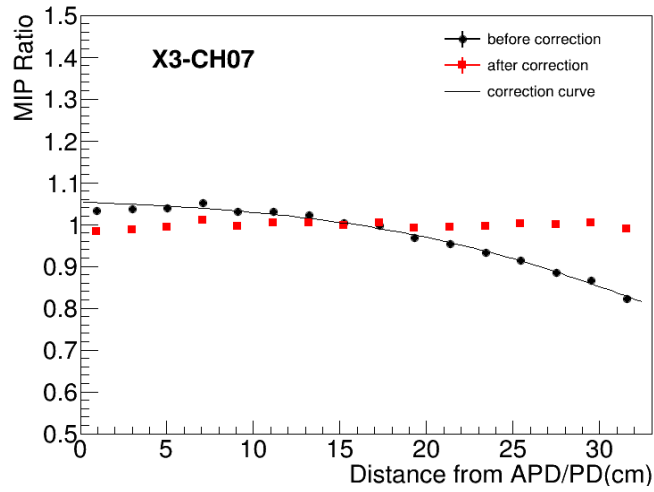
Distribution of deposit energies (ΔE) in TASC



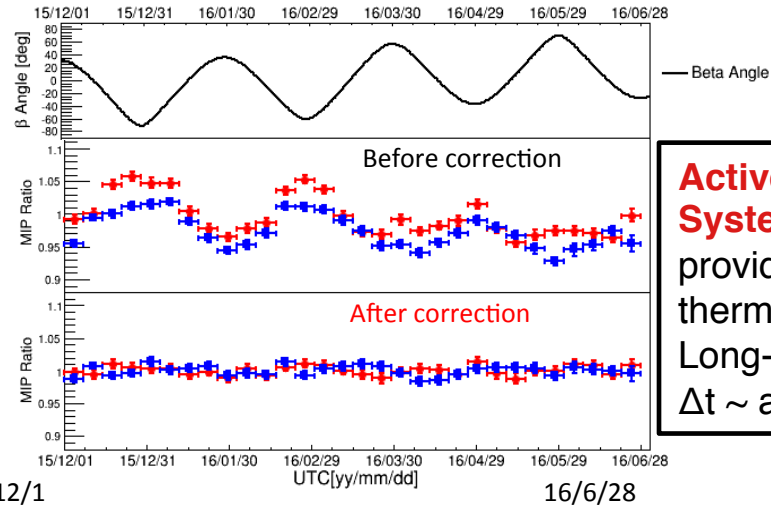


Position and Temperature Calibration + Long-term Stability

Example of **position dependence** correction



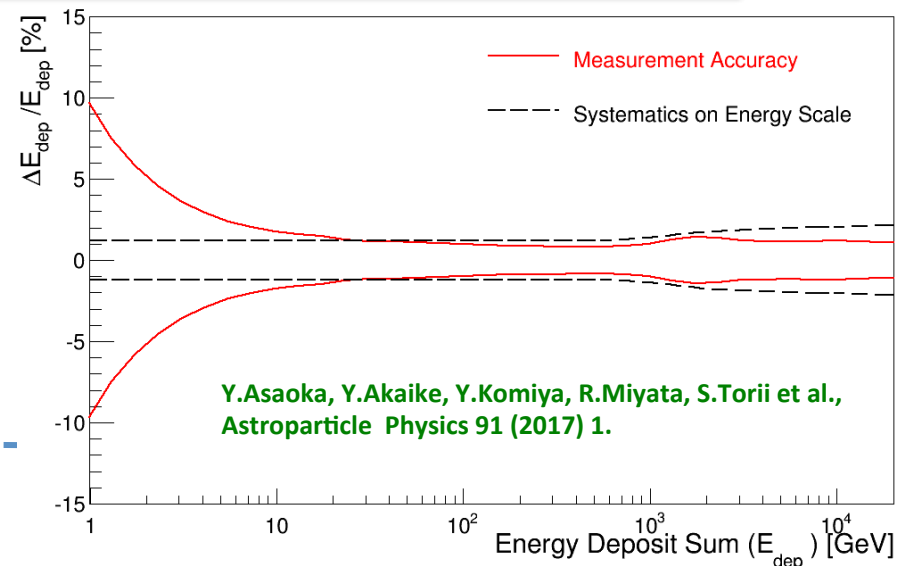
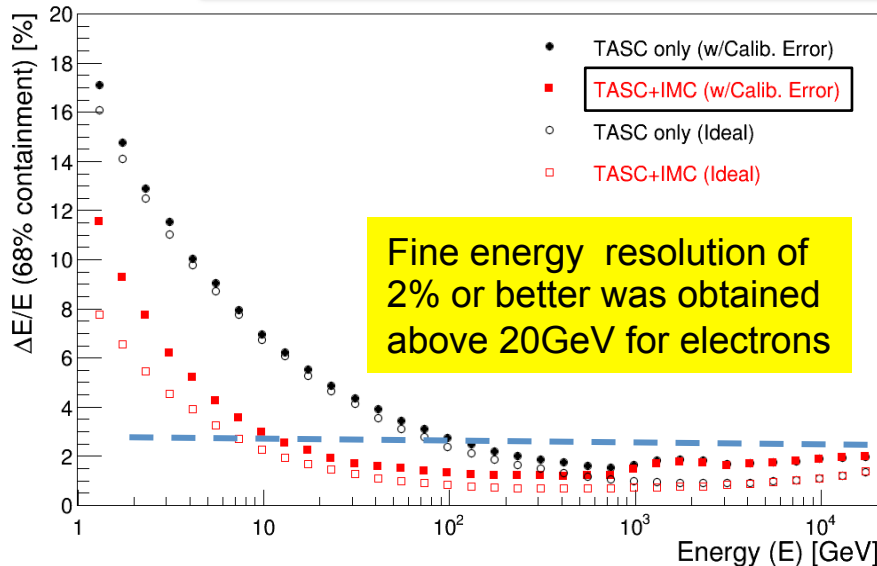
Examples of **temperature change** correction



TASC

Active Thermal Control System (ATCS) on ISS provides very stable thermal condition during Long-term observations: $\Delta t \sim$ a few degrees

Energy Resolution for Electrons by On-orbit Calibration



Y.Asaka, Y.Akaike, Y.Komiya, R.Miyata, S.Torii et al., *Astroparticle Physics* 91 (2017) 1.



Simple Two Parameter Cut

F_E : Energy fraction of the bottom layer sum to the whole energy deposit sum in TASC
 R_E : Lateral spread of energy deposit in TASC-X1

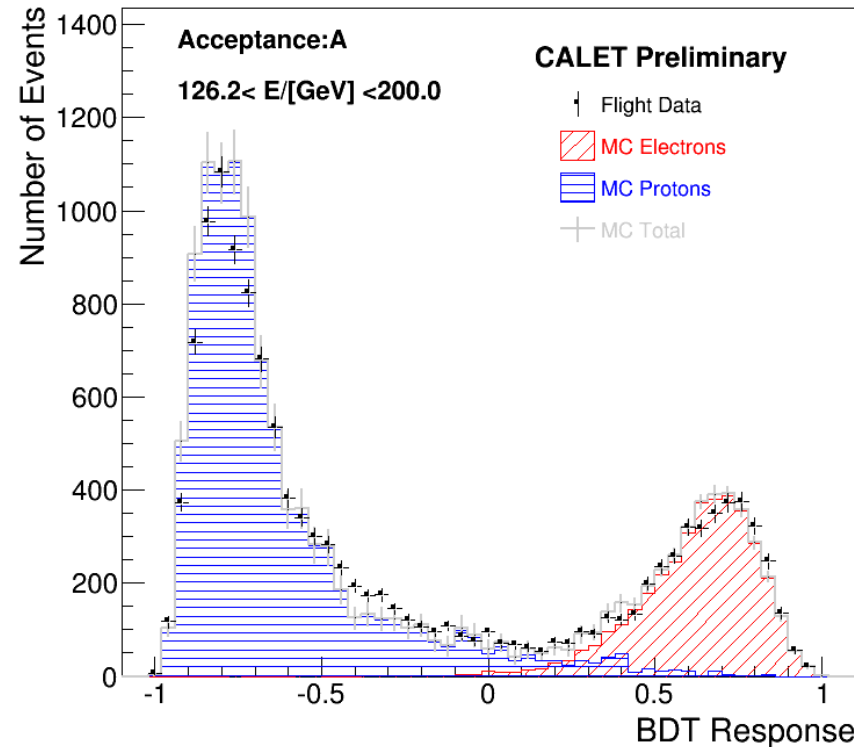
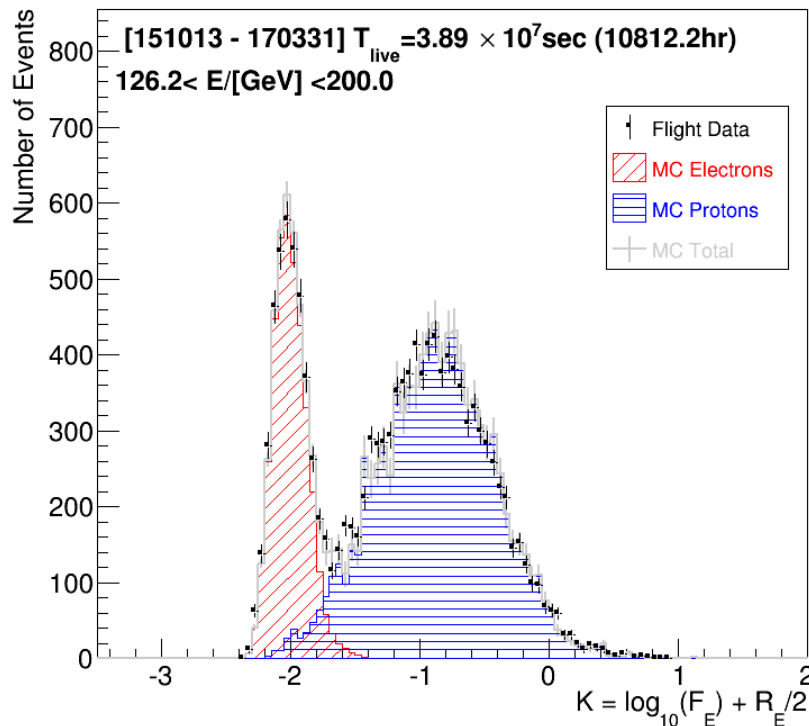
Cut Parameter K is defined as follows:

$$K = \log_{10}(F_E) + R_E/2$$

Boosted Decision Trees (BDT)

In addition to the two parameters on the left, TASC and IMC shower profile fits are used as discriminating variables

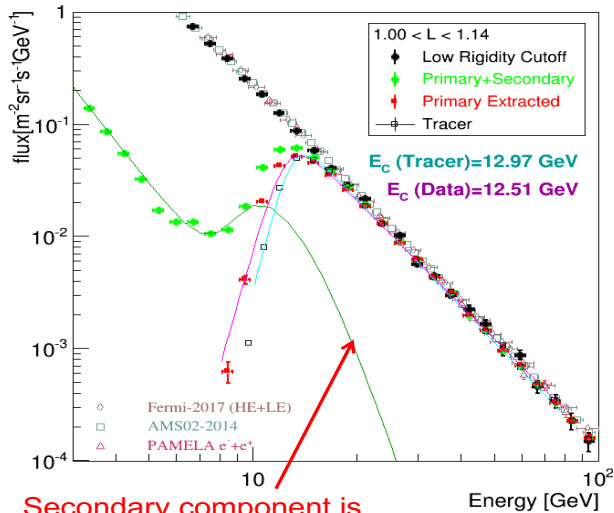
BDT Response using 9 parameters





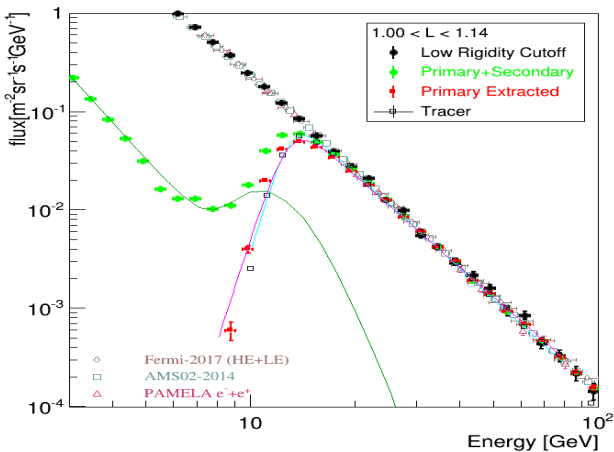
Cutoff Rigidity Measurements and Comparison with Calculation

BEFORE CORRECTION

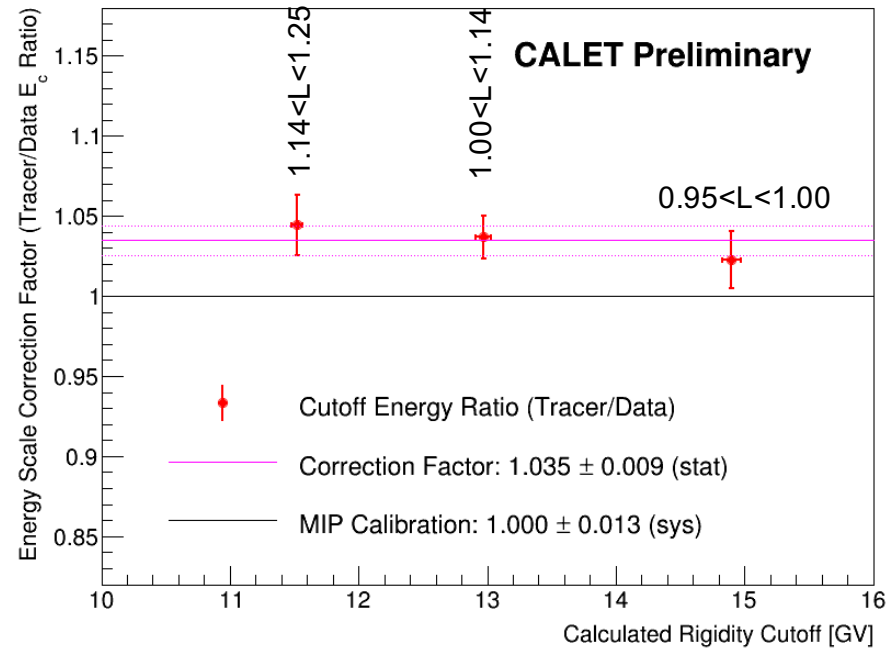


Secondary component is estimated using azimuthal distributions

AFTER CORRECTION



- Performed in three different cutoff rigidity regions.
- Correction factor was found to be **1.035** compared to MIP calibration.



[Y.Asaoka, COSPAR 2018 E1.5-0023-18]

[S.Miyake, COSPAR 2018 E1.5-0027-18]



Systematic Uncertainties in Derivation of Energy Spectrum

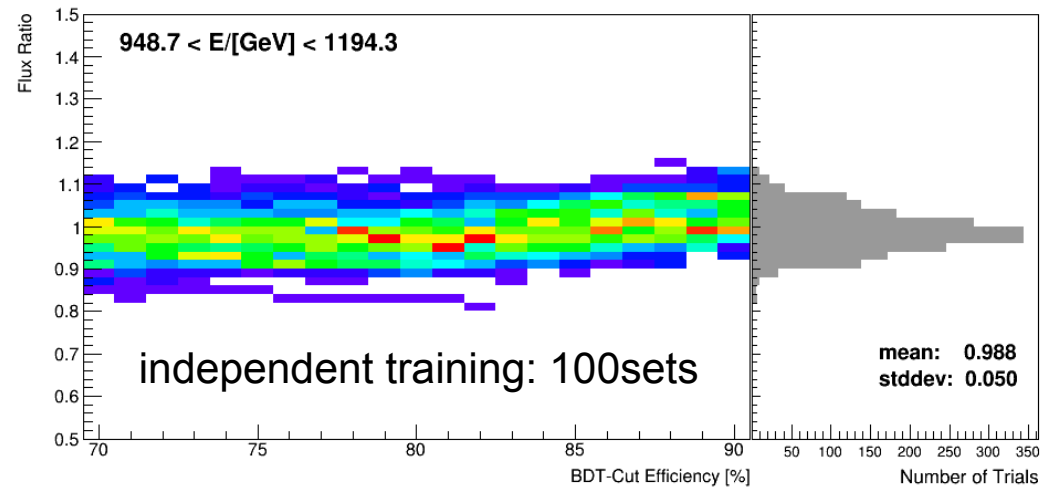
The stability of the measured flux is intensively studied in the large parameter space of analysis selection criteria, including:

- Normalization:
 - Live time
 - Radiation environment
 - Long-term stability
 - Quality cuts
- Energy dependent:
 - Tracking
 - charge ID
 - electron ID (K-Cut vs BDT)
 - BDT stability (vs efficiency & training)
 - MC model (EPICS vs Geant4)

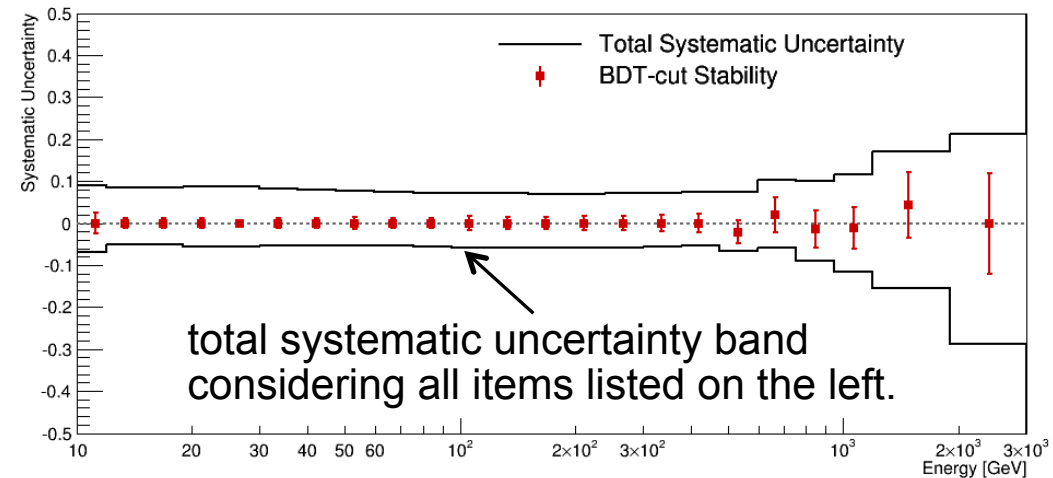
N.B. Energy scale uncertainty is not included in this analysis.

[Y.Asaoka, COSPAR 2018 E1.5-0023-18]

Systematic uncertainty in electron selection by BDT



Total systematic uncertainty vs Energy

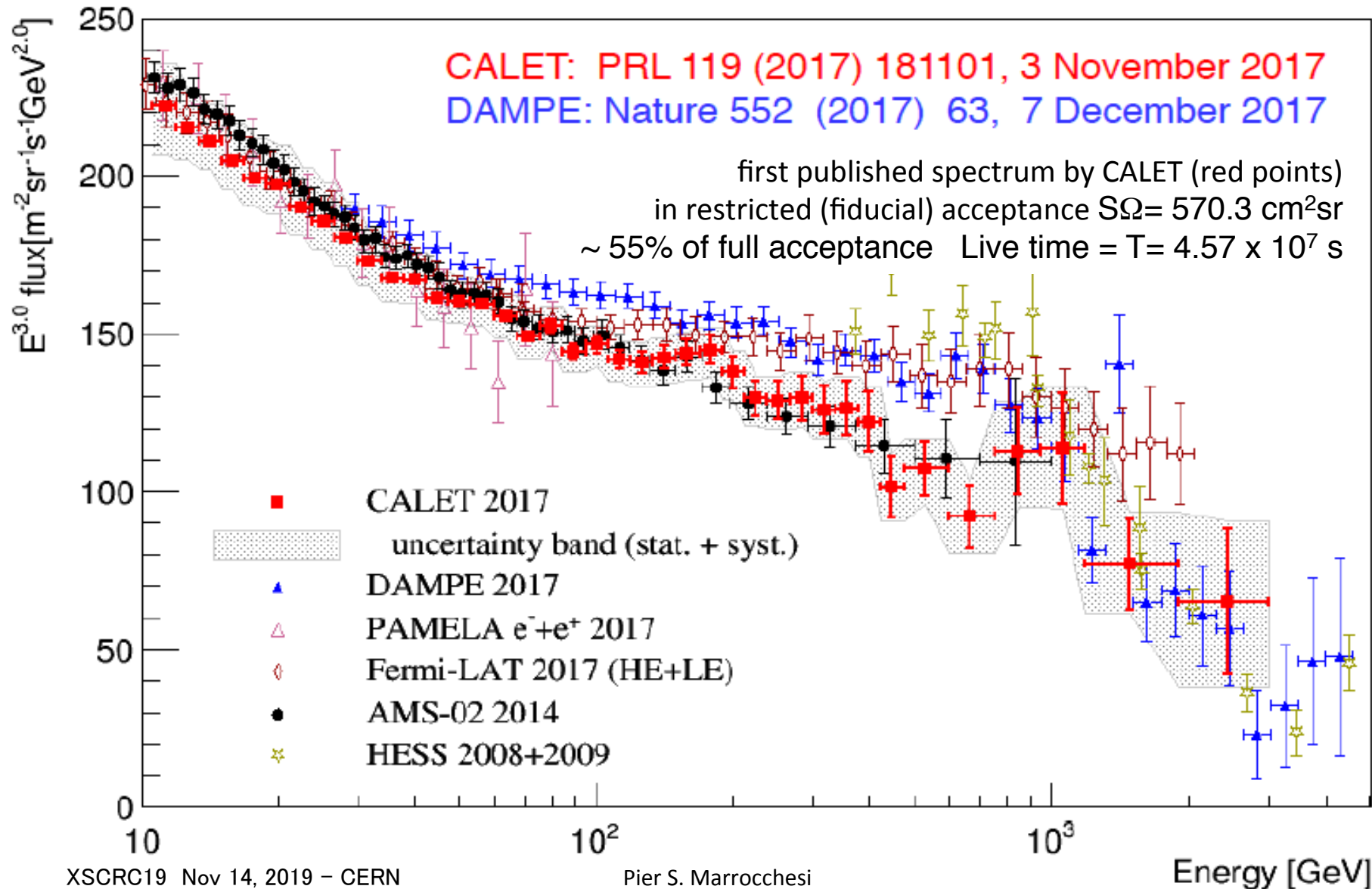


ELECTRONS + POSITRONS



Direct measurements of the electron spectrum

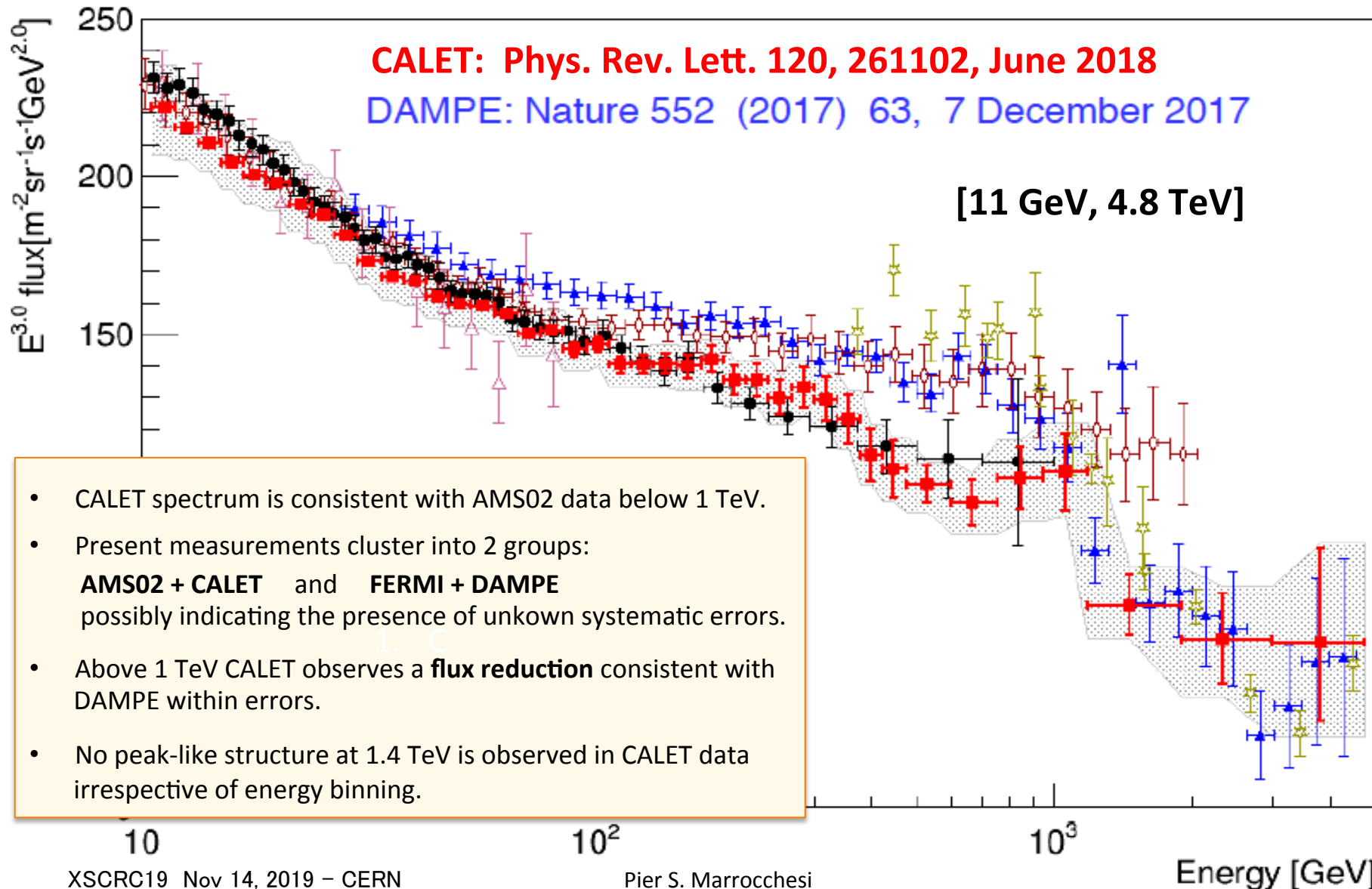
Comparison of CALET with DAMPE and other experiments in space





Extended CALET measurement of **electron** spectrum

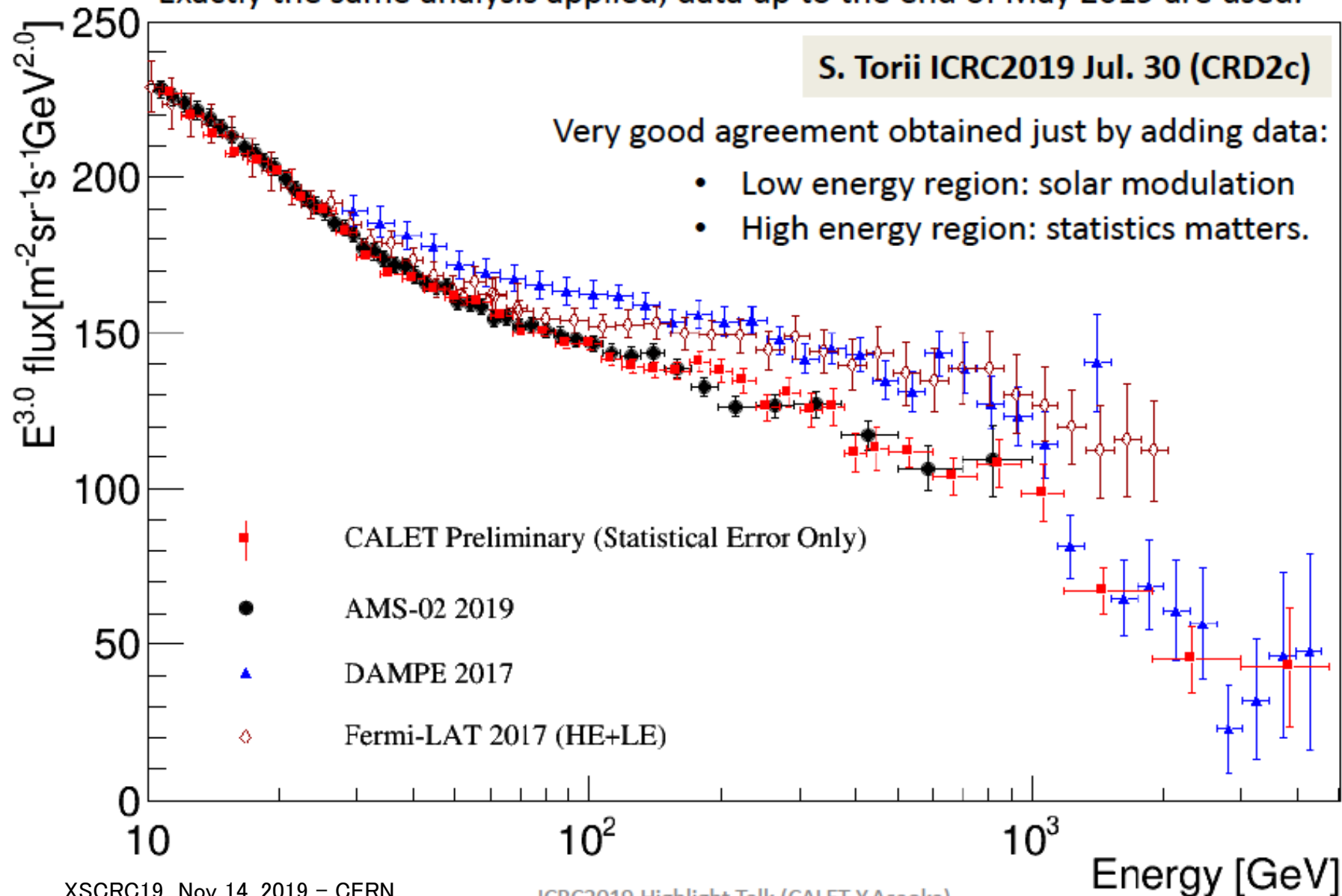
Approximately doubled statistics above 500GeV by using full acceptance of CALET





All Electron Spectrum: Comparison between updated AMS-02 & CALET

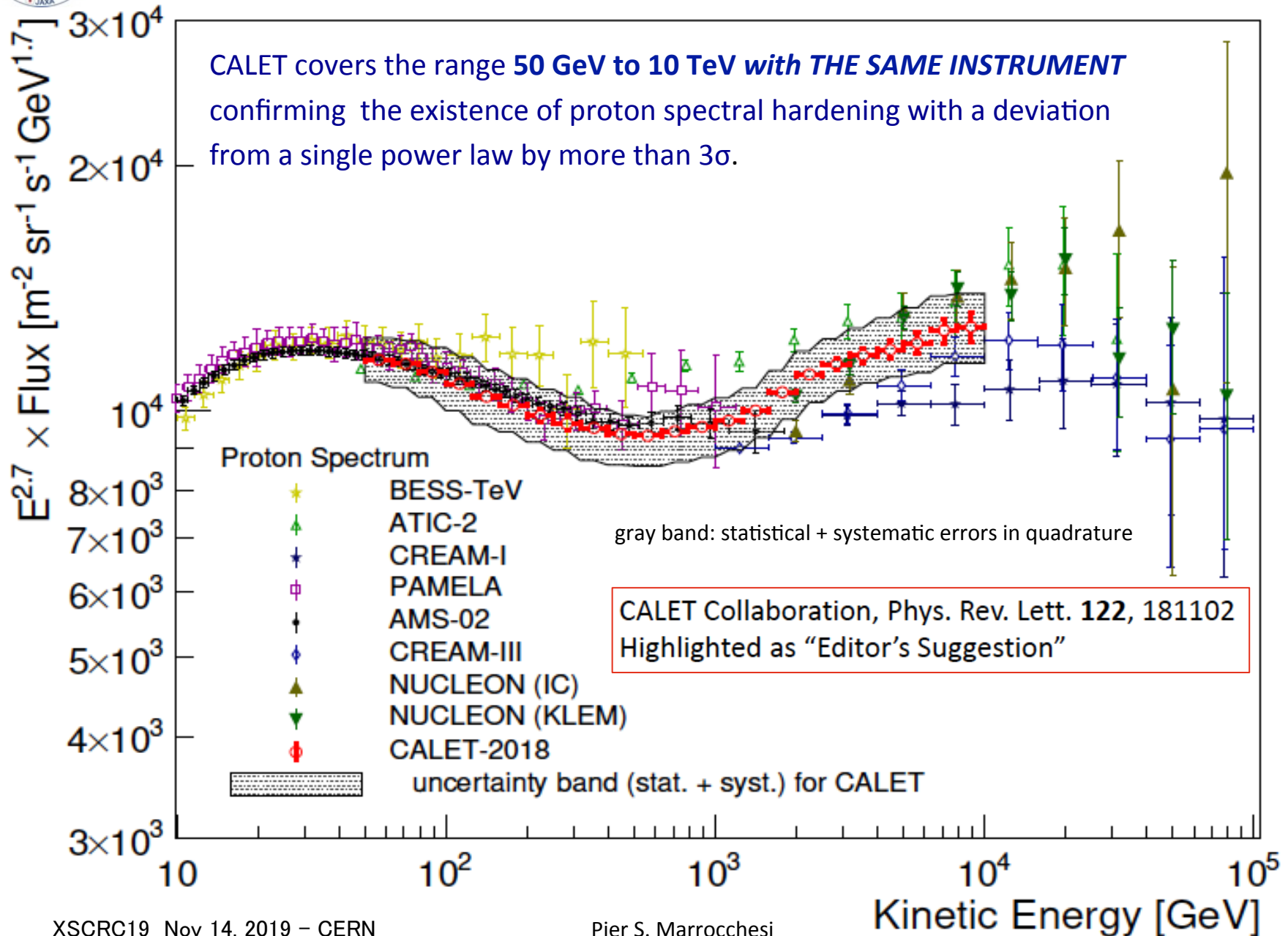
Exactly the same analysis applied, data up to the end of May 2019 are used.



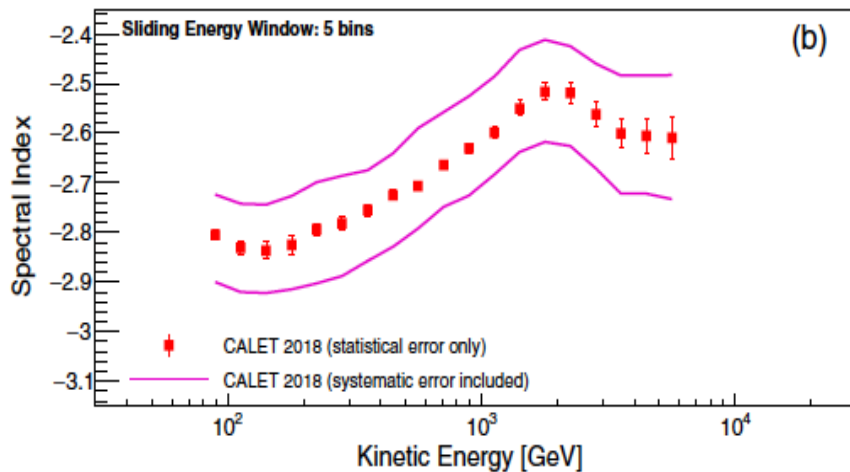
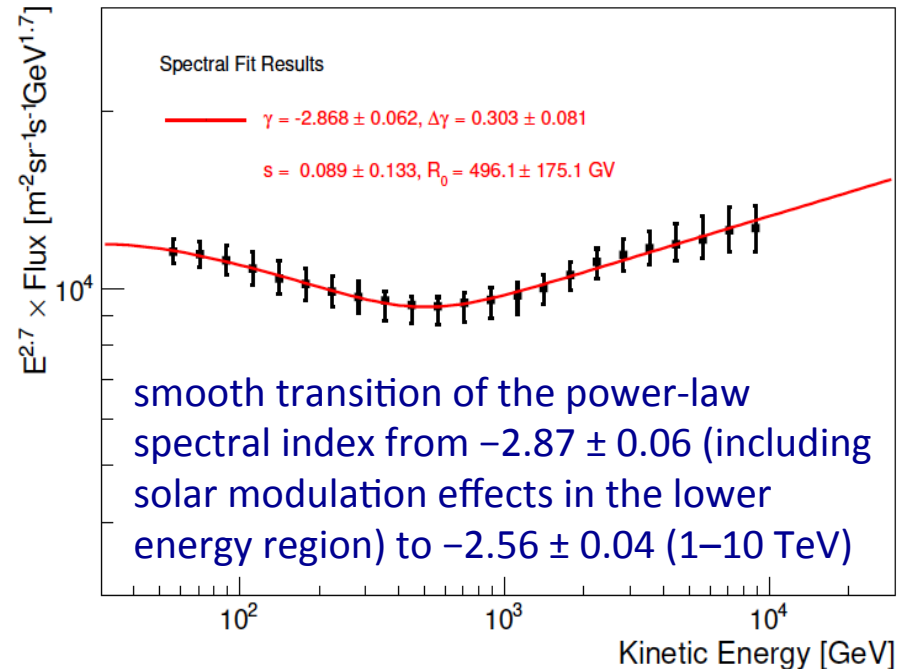
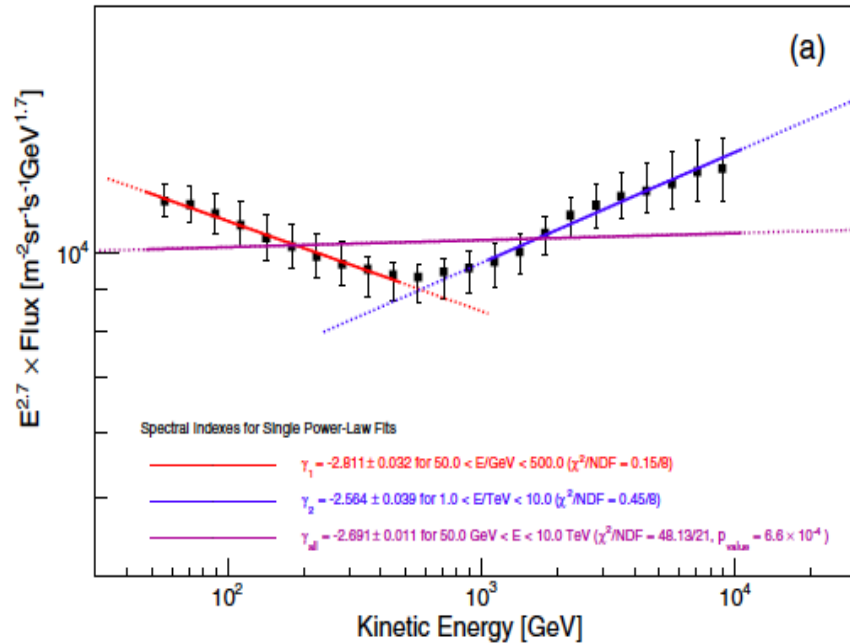
PROTONS



Direct measurement of **proton** spectrum by CALET



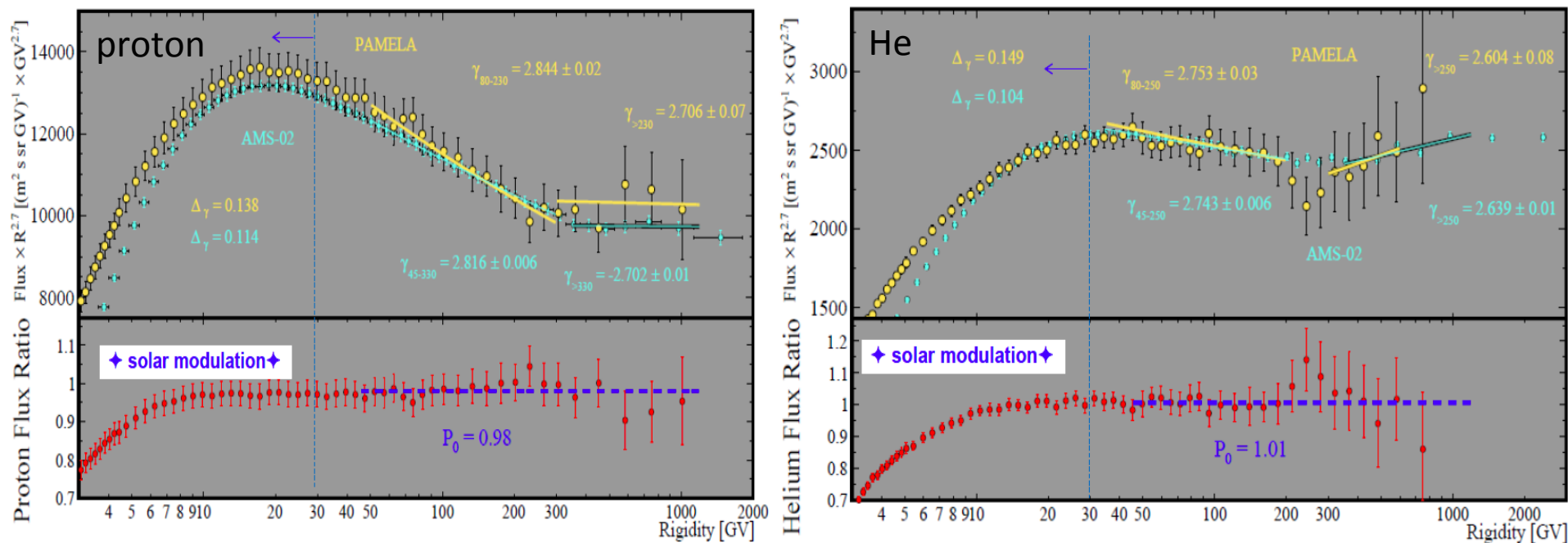
Spectral Behavior of Proton Flux



1. Subranges of 50—500GeV, 1-10TeV can be fitted with single power law function, but not the whole range (significance $> 3\sigma$).
2. Progressive hardening up to the TeV region was observed.
3. “smoothly broken power-law fit” gives power law index consistent with AMS-02 in the low energy region, but shows larger index change and higher break energy than AMS-02.

New era of precision spectral measurements:

- ✧ **p and He below 100 GeV:** % level agreement of magnetic spectrometers (BESS-TeV, PAMELA, AMS02)
- ✧ good agreement of PAMELA and AMS-02 on p and He spectra **below a few hundred GeV**



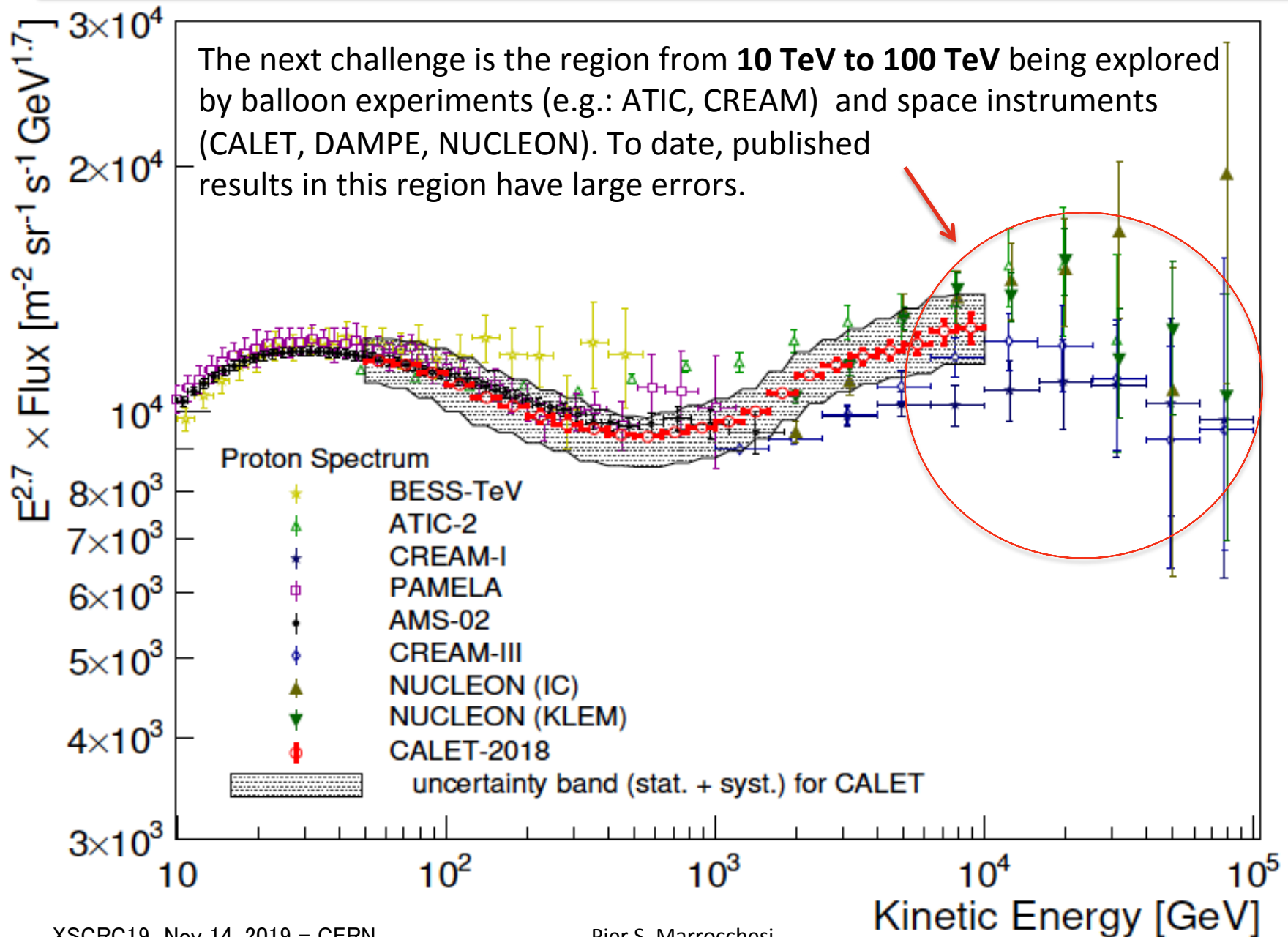
[M.Boezio @LNGS Jul 2016]

O. Adriani et al., Phys. Rep. 544 (2014) 323; M. Aguilar et al., PRL 114 (2015) 171103

O. Adriani et al., Science 332 (2011) 6025; M. Aguilar et al., PRL 115, (2015) 211101

	fit range proton	γ_p	fit range He	γ_{He}
PAMELA	80-230 GV	-2.844 ± 0.02	80-250 GV	-2.753 ± 0.03
AMS-02	45-330 GV	-2.816 ± 0.006	45-250 GV	-2.743 ± 0.006

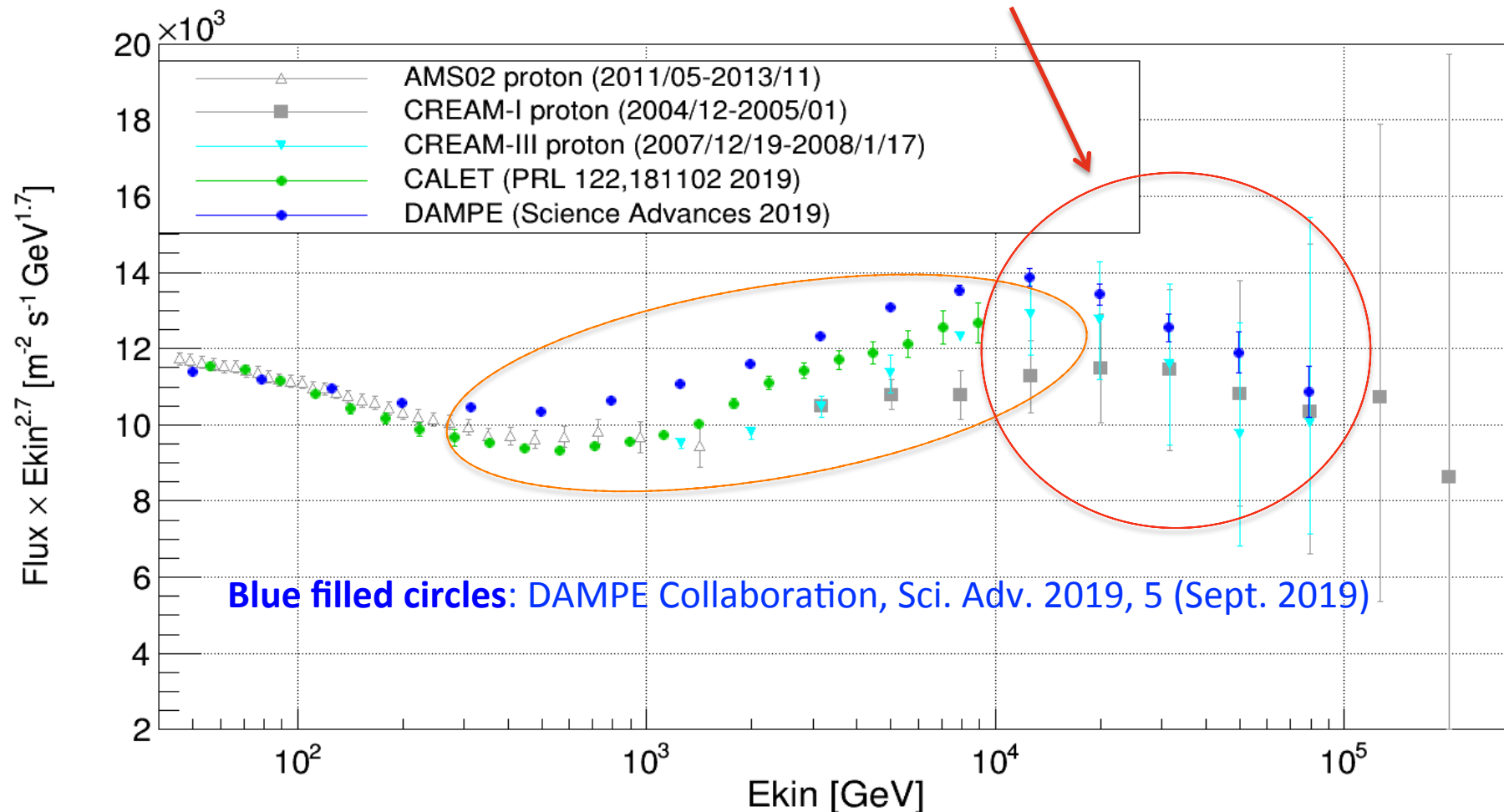
Direct measurements of p spectrum before Sept 2019



RECENT direct measurements of proton spectrum

Recent paper by DAMPE collaboration (Sept 2019) from 40 GeV to 100 TeV:

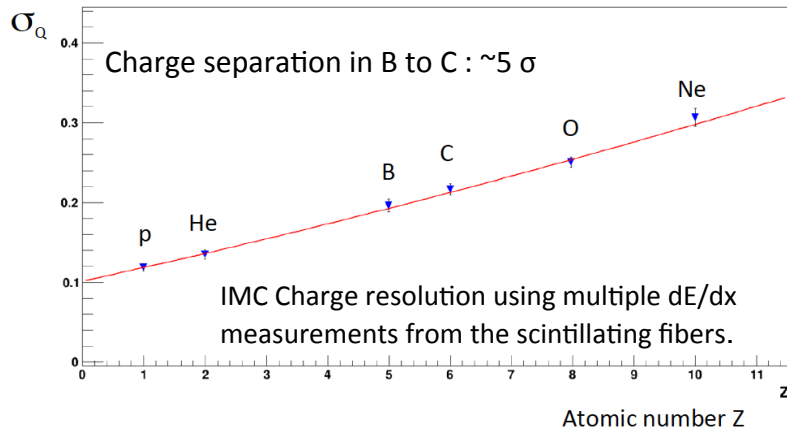
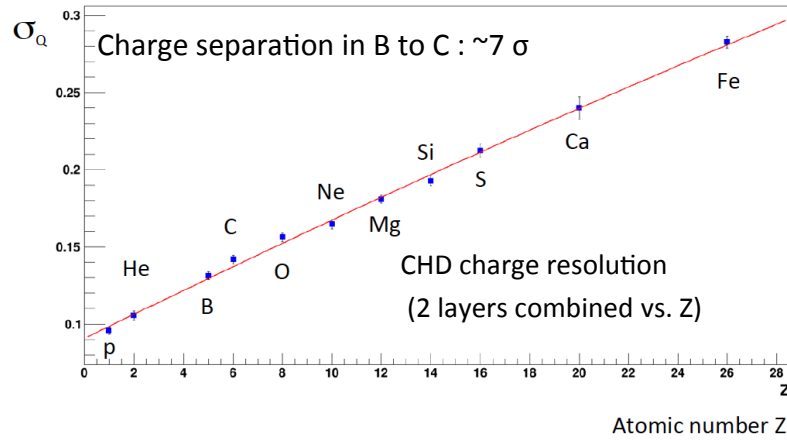
- flux higher than AMS02 and CALET above 200 – 300 GeV
- flux higher than CREAM-III (and CREAM-I) in the region 1 TeV to 10 TeV approx.
- flux reduction above 13.6 TeV (spectral index changes from ~ 2.60 to ~ 2.85)





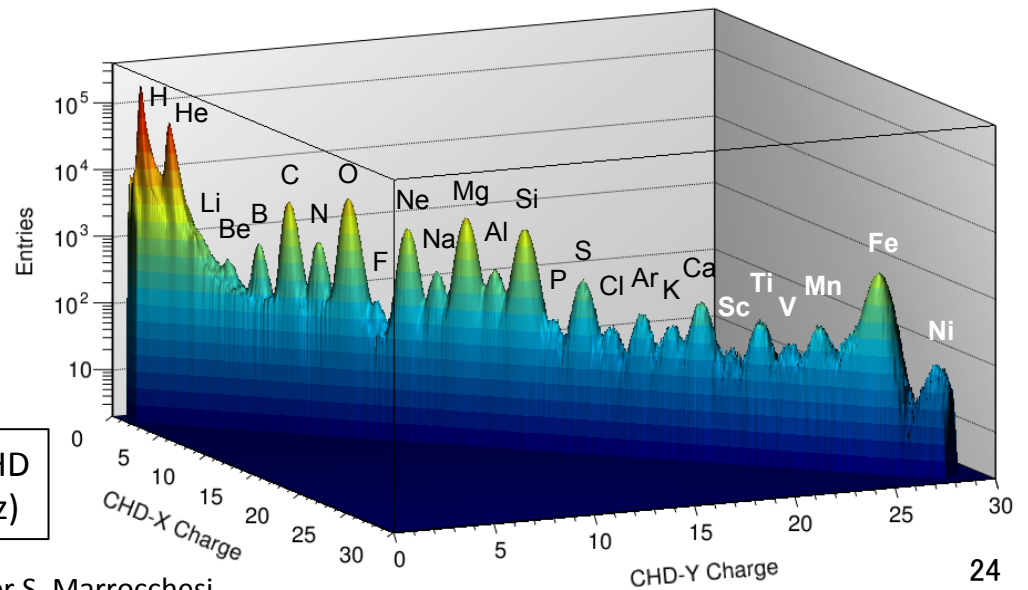
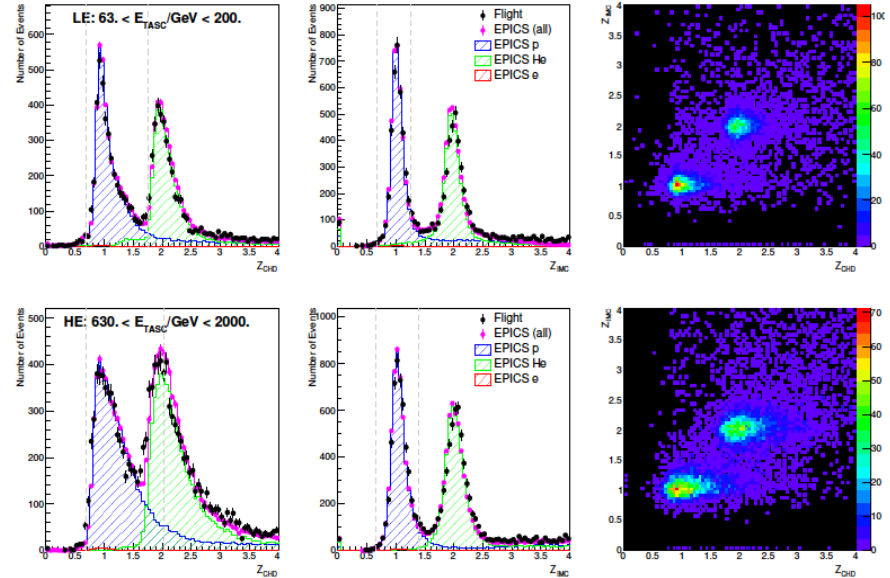
Charge Identification of Nuclei with CHD and IMC

Single element selection for p, He and light nuclei is achieved by CHD+IMC charge analysis.



Deviation from Z^2 response is corrected both in CHD and IMC using a core + halo ionization model (Voltz)

Combined CHD-IMC proton-Helium charge-ID



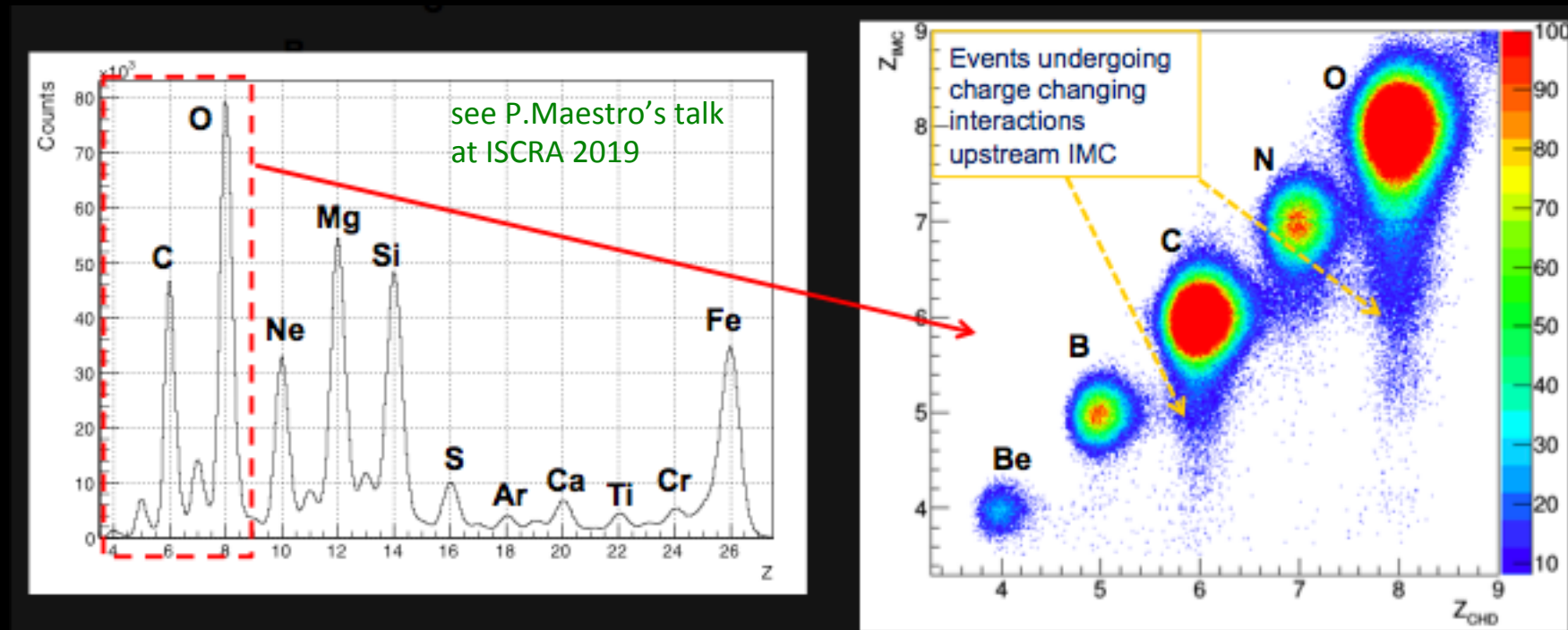


Observation of Light Nuclei

- CALET can identify **individual elements** thanks to the redundant charge determination in CHD and IMC and the excellent charge resolution.

Left: well resolved charge peaks from Be to Fe (all plots are in units of atomic number Z)

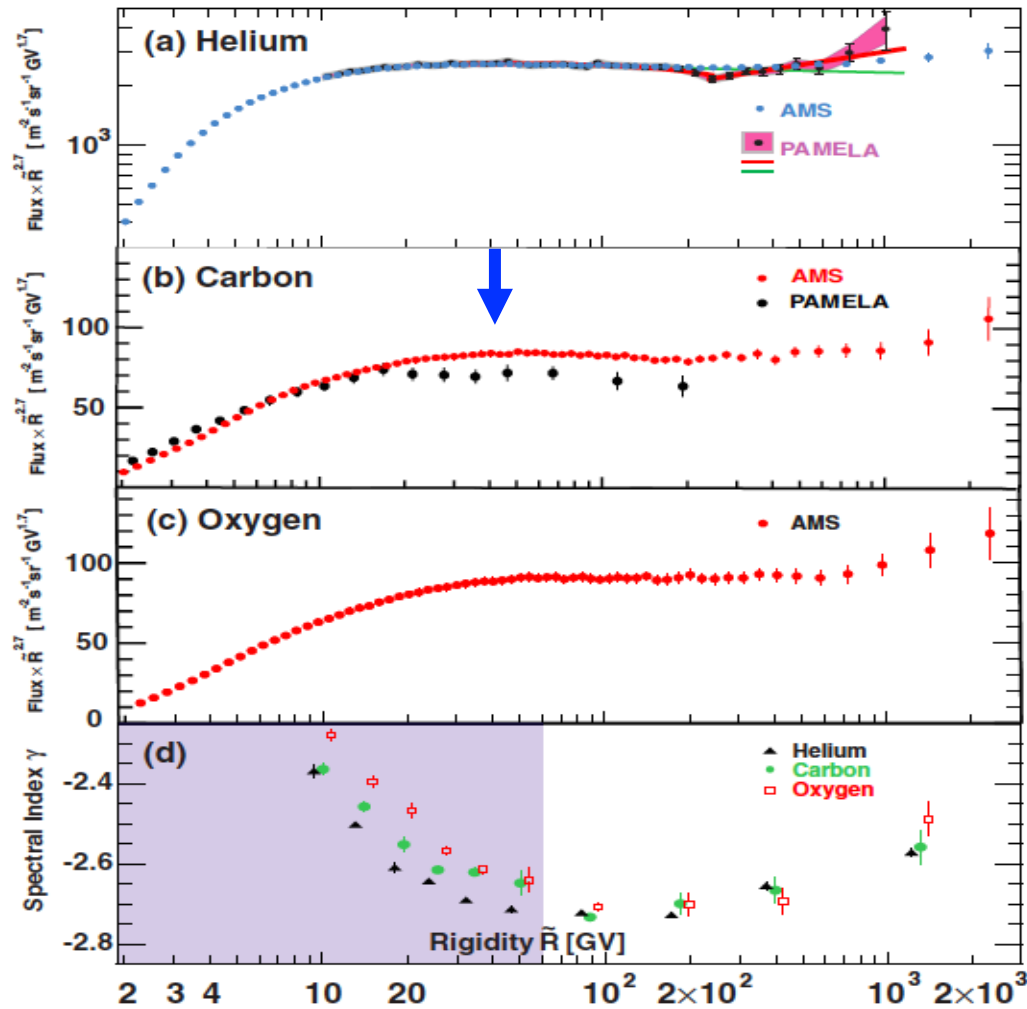
Right: Scatter plot of IMC vs CHD charge



Light Primaries: Carbon and Oxygen

fluxes vs Rigidity from PAMELA and AMS

2018



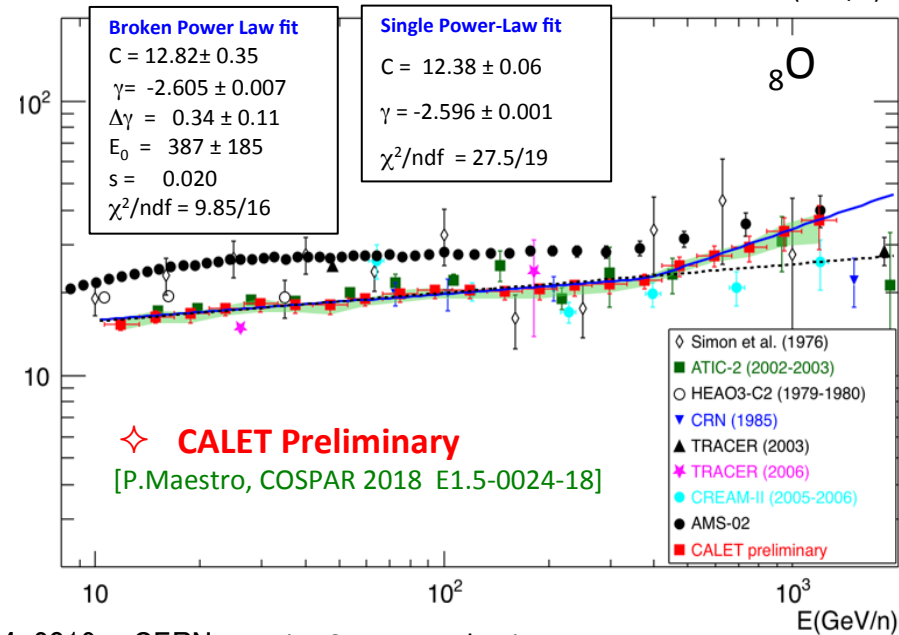
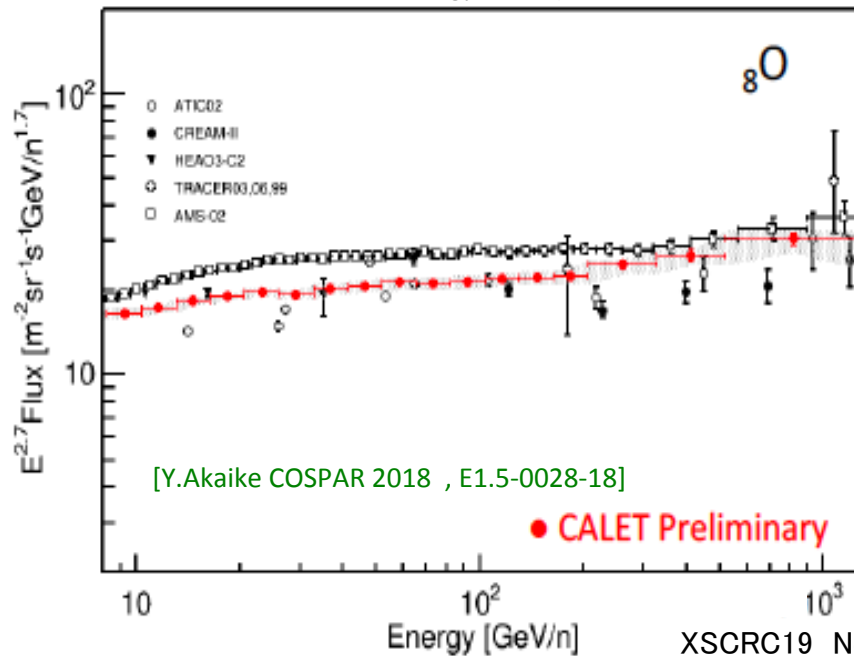
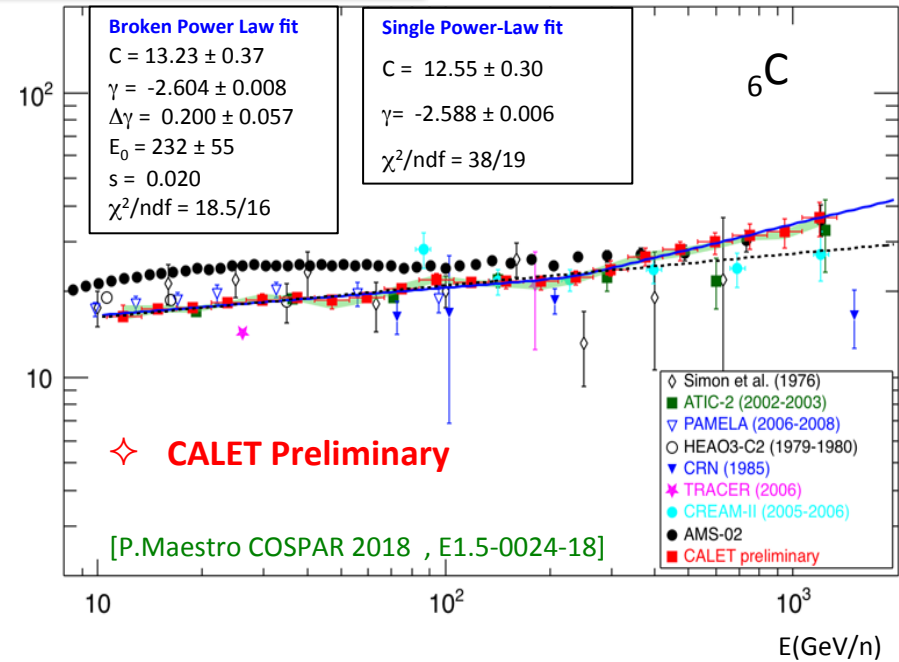
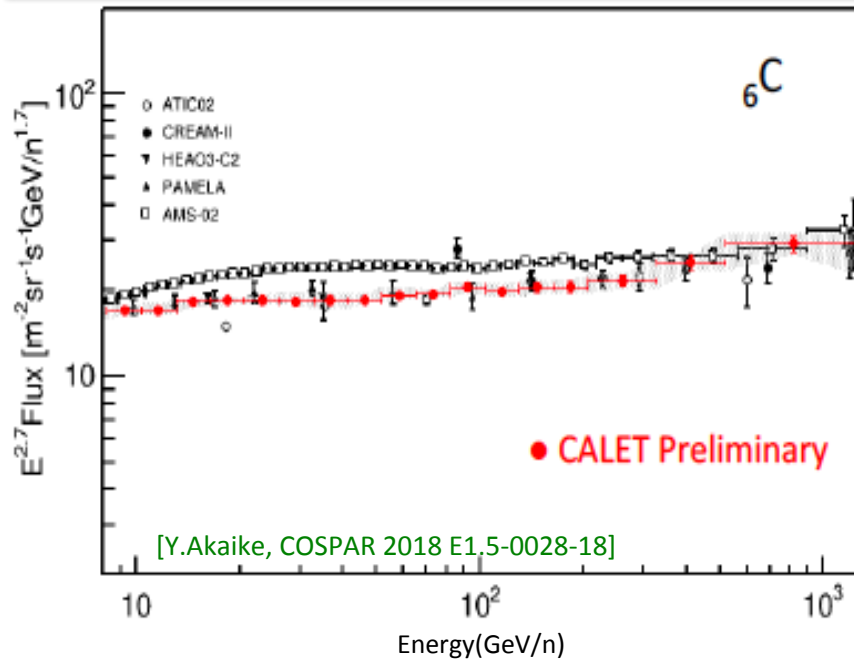
above ~ 10 GV AMS
carbon flux is $\sim 15\%$
higher than PAMELA

no published data
for oxygen flux
by PAMELA

Rigidity (GV)

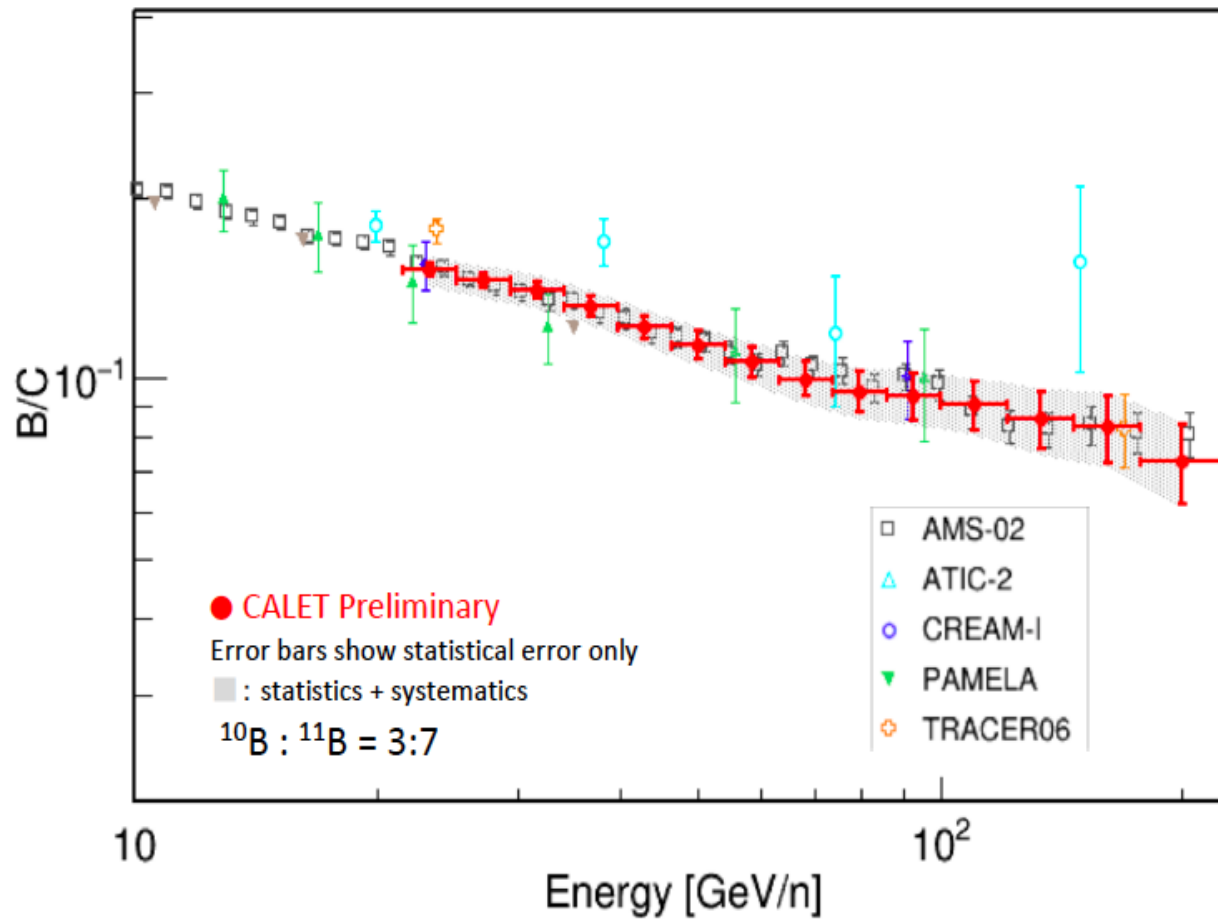
NUCLEI

Preliminary Energy spectra of Carbon and Oxygen (2 independent CALET analyses)





Boron-to-carbon flux ratio (Preliminary)



[Y. Akaike, APS April 14, 2019]

$$^{10}\text{B} : ^{11}\text{B} = 3:7$$

Source of systematic uncertainties

- Trigger efficiency
- Charge consistency cuts
- Track width selection
- Window range for charge identification
- Background model of p and He spectra
- Initial assuming spectra for energy unfolding
- Energy correction base on beam test results
- Difference of beam test model and flight model
- Long term stability



Preliminary Flux of Primary Components

Flux measurements:

$$\Phi(E) = \frac{N(E)}{S\Omega\epsilon(E)T\Delta E}$$

$N(E)$: Events in unfolded energy bin

$S\Omega$: Geometrical acceptance

$\epsilon(E)$: Efficiency

T : Live Time

ΔE : Energy bin width

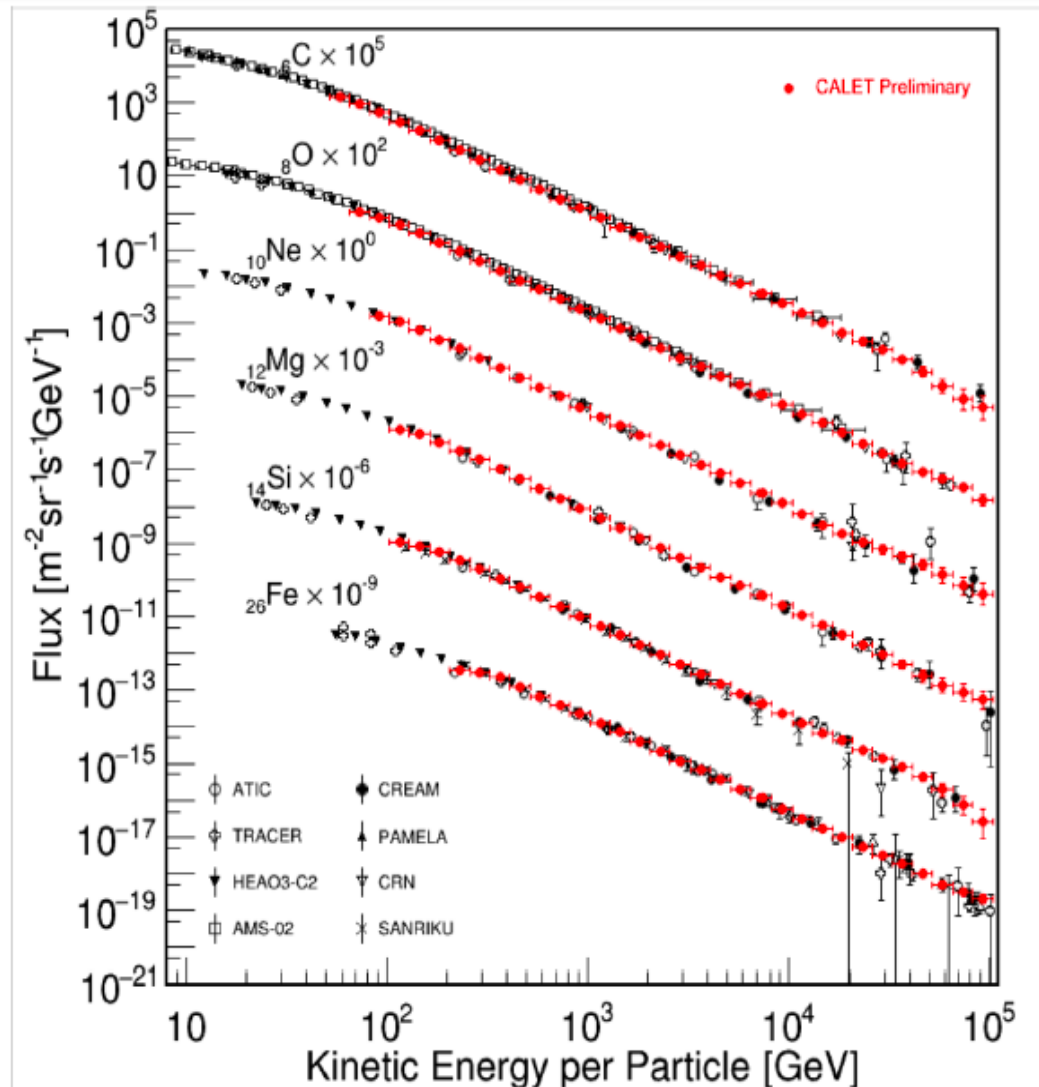
Observation period:

Oct.13 2015 – May.31 2018

(962 days)

5.6×10^6 events (C-Fe, $\Delta E > 10$ GeV)

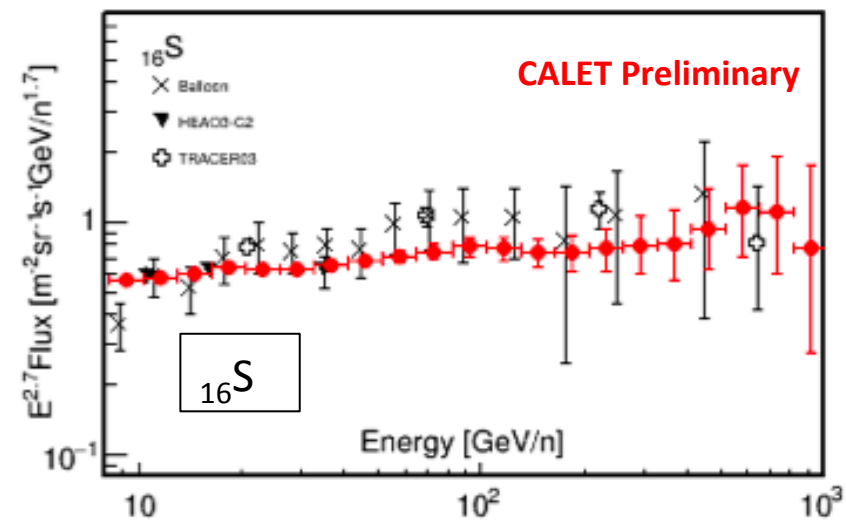
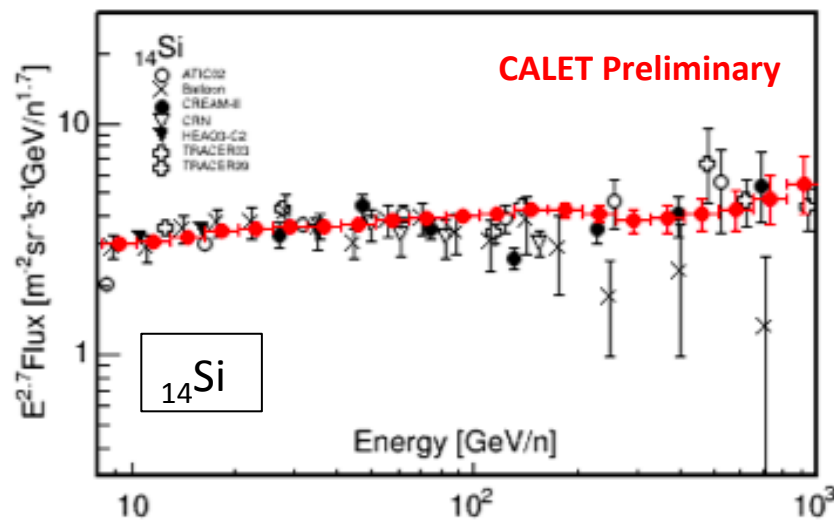
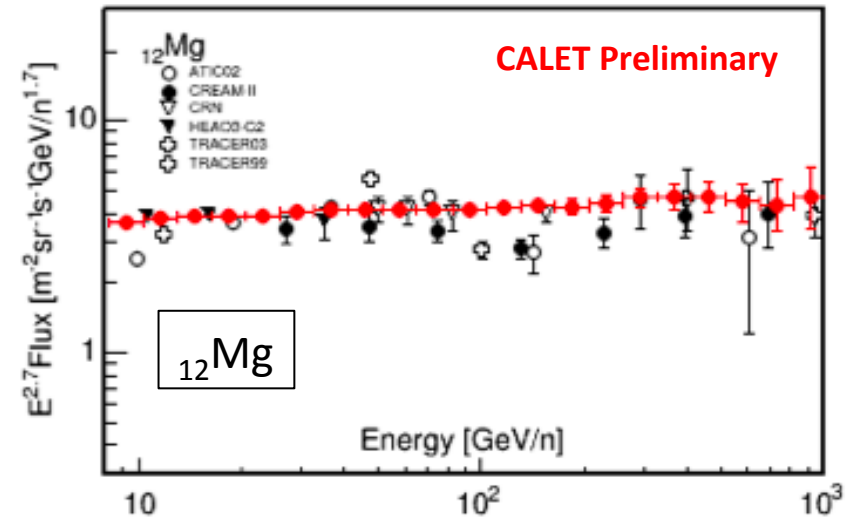
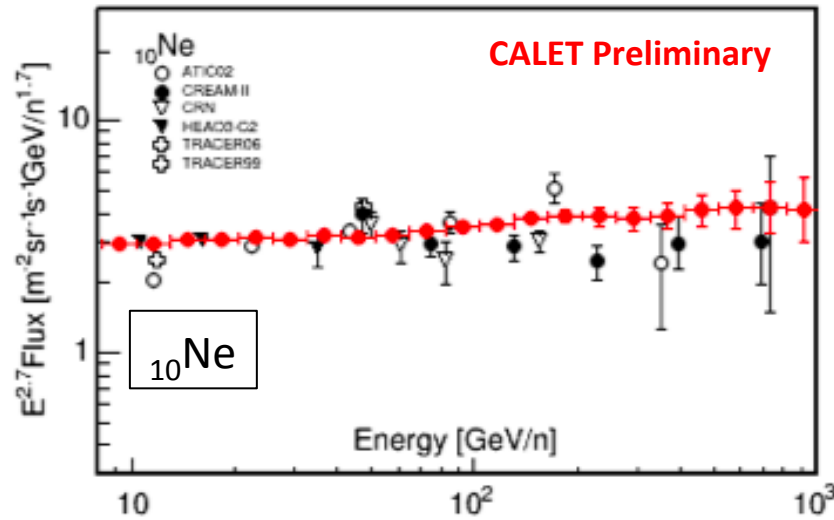
[Y. Akaike, APS April 14, 2019]





Preliminary Spectra of Z-even Nuclei from Ne to S (Z = 10-16)

[Y.Akaike, COSPAR 2018 E1.5-0028-18]

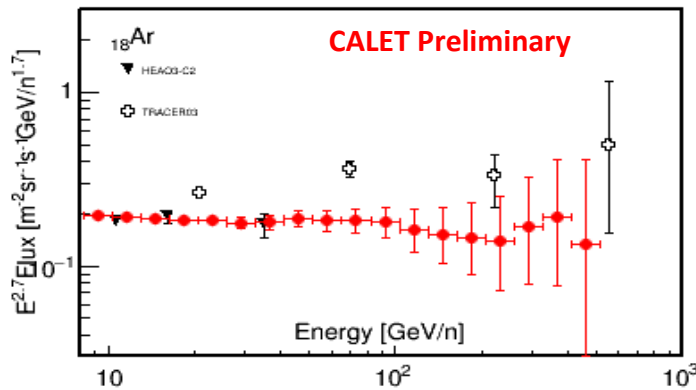




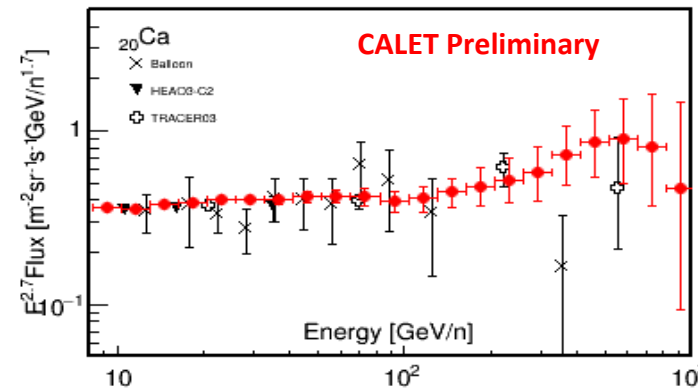
Preliminary Spectra of Z-even Nuclei from Ar to Ni (Z = 18-28)

[Y.Akaike, COSPAR 2018 E1.5-0028-18]

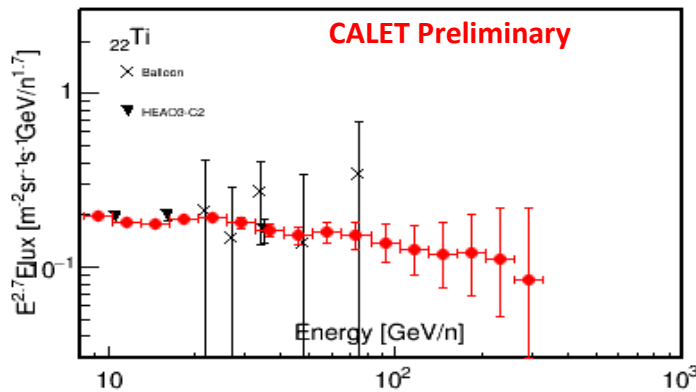
^{18}Ar



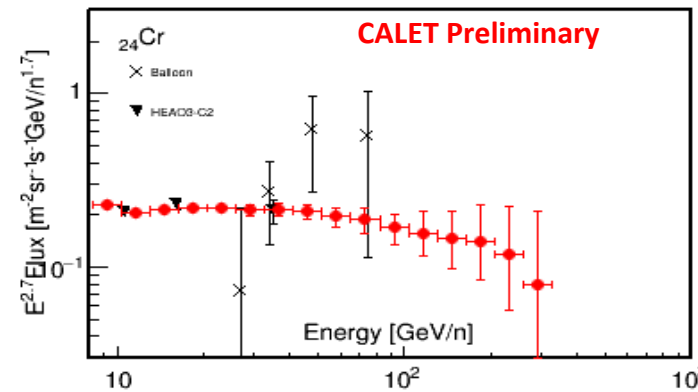
^{20}Ca



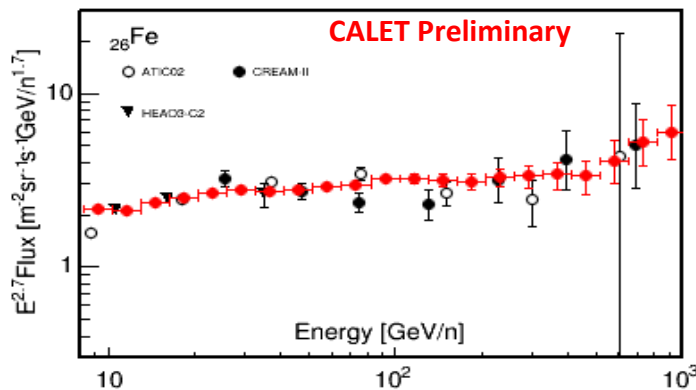
^{22}Ti



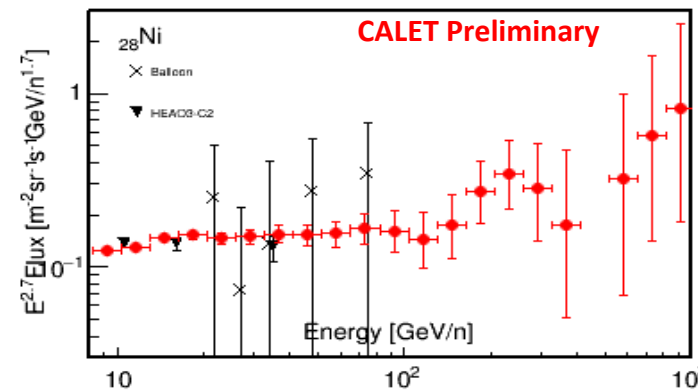
^{24}Cr



^{26}Fe



^{28}Ni





Ultra Heavy Nuclei (Preliminary Measurements for $26 < Z \leq 40$)

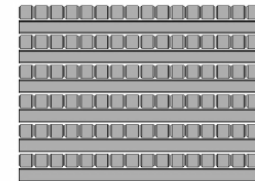
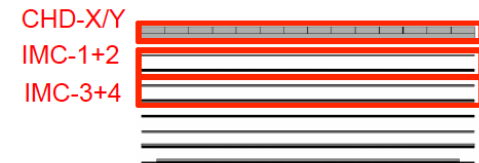
[B.Rauch, APS April 14, 2019]

CALET measures the relative abundances of nuclei above Fe through ${}_{40}\text{Zr}$

CALET has a special UH CR trigger utilizing the CHD and the top 4 layers of the IMC that:

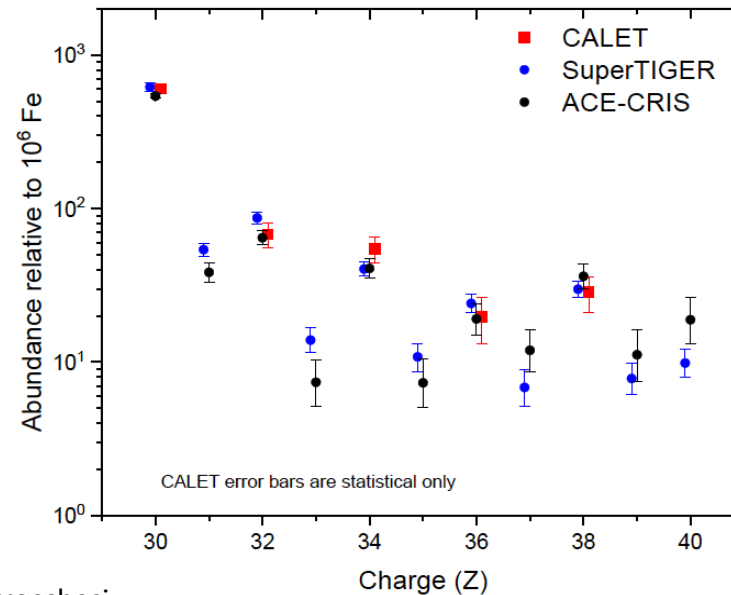
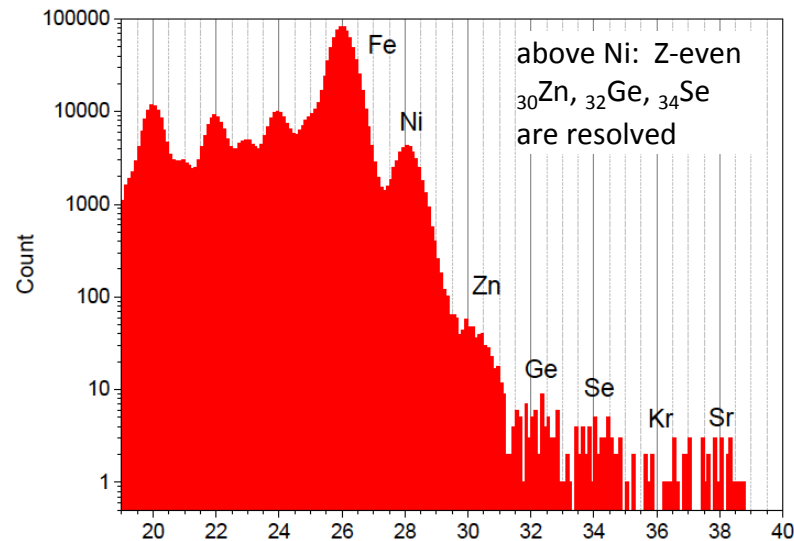
- has an expanded geometry factor of $\sim 4000 \text{ cm}^2\text{sr}$
- has a very high duty cycle due to low event rate

Onboard trigger for UH events



Data analysis

- Event Selection: Vertical cutoff rigidity $> 4\text{GV}$ & Zenith Angle < 60 degrees
- Contamination from neighboring charge are determined by multiple-Gaussian fit
- ◇ The CALET UH element ratios relative to ${}_{26}\text{Fe}$ show good agreement with SuperTIGER and ACE abundances.





CALET γ -ray Sky ($>1\text{ GeV}$)

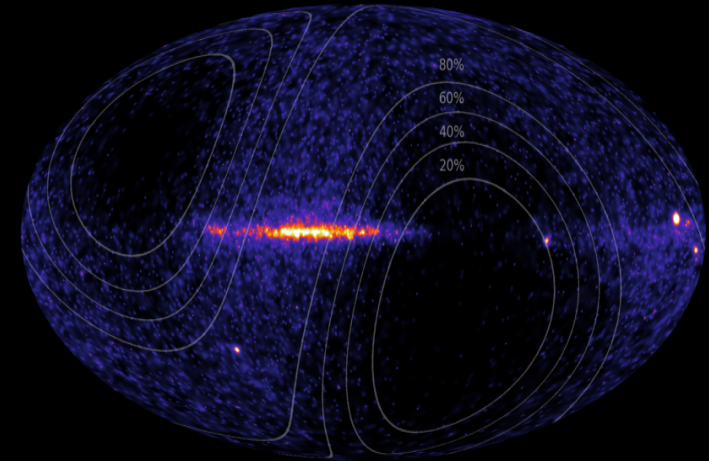
Instrument characterized using EPICS simulations

- Effective area $\sim 400\text{ cm}^2$ above 2 GeV
- Angular resolution $< 2^\circ$ above 1 GeV ($< 0.2^\circ$ above 10 GeV)
- Energy resolution $\sim 12\%$ at 1 GeV ($\sim 5\%$ at 10 GeV)

Simulated IRFs consistent with 2 years of flight data

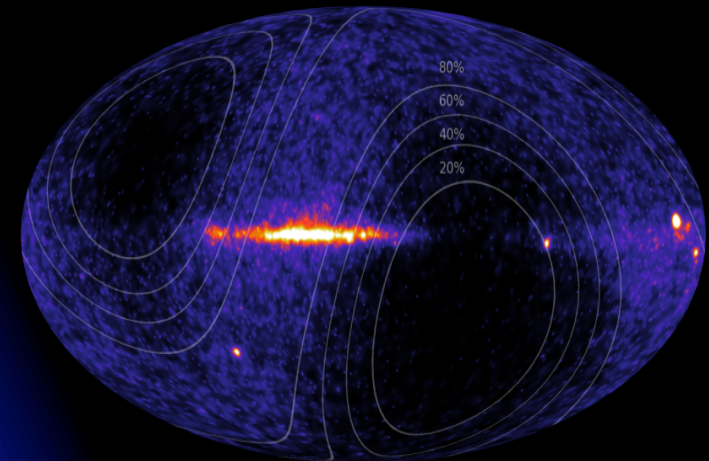
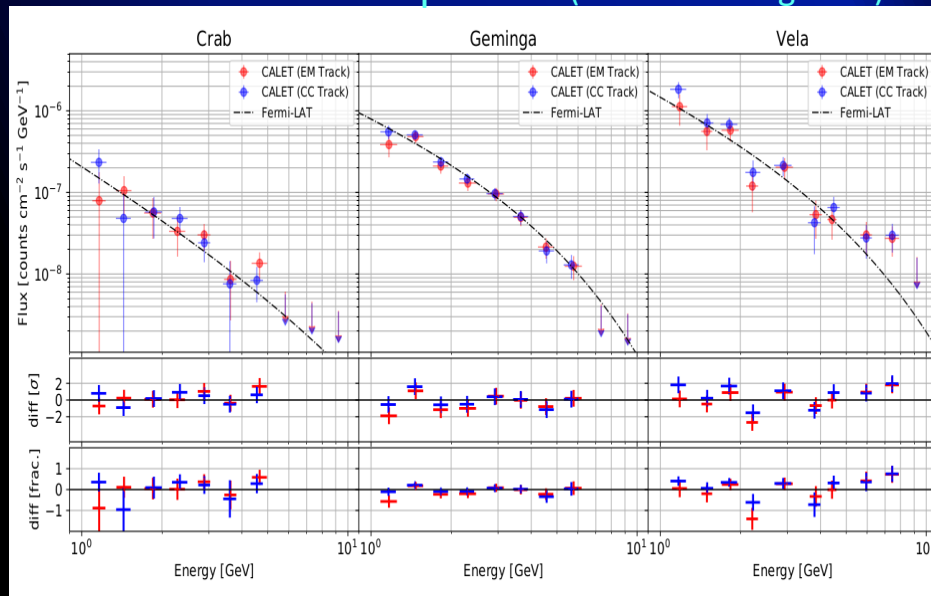
Consistency in signal-dominated regions with Fermi-LAT

Residual background in low-signal regions



[N.Cannady, COSPAR 2018 E1.17-0009-18]

Flux validation with pulsars (under investigation)

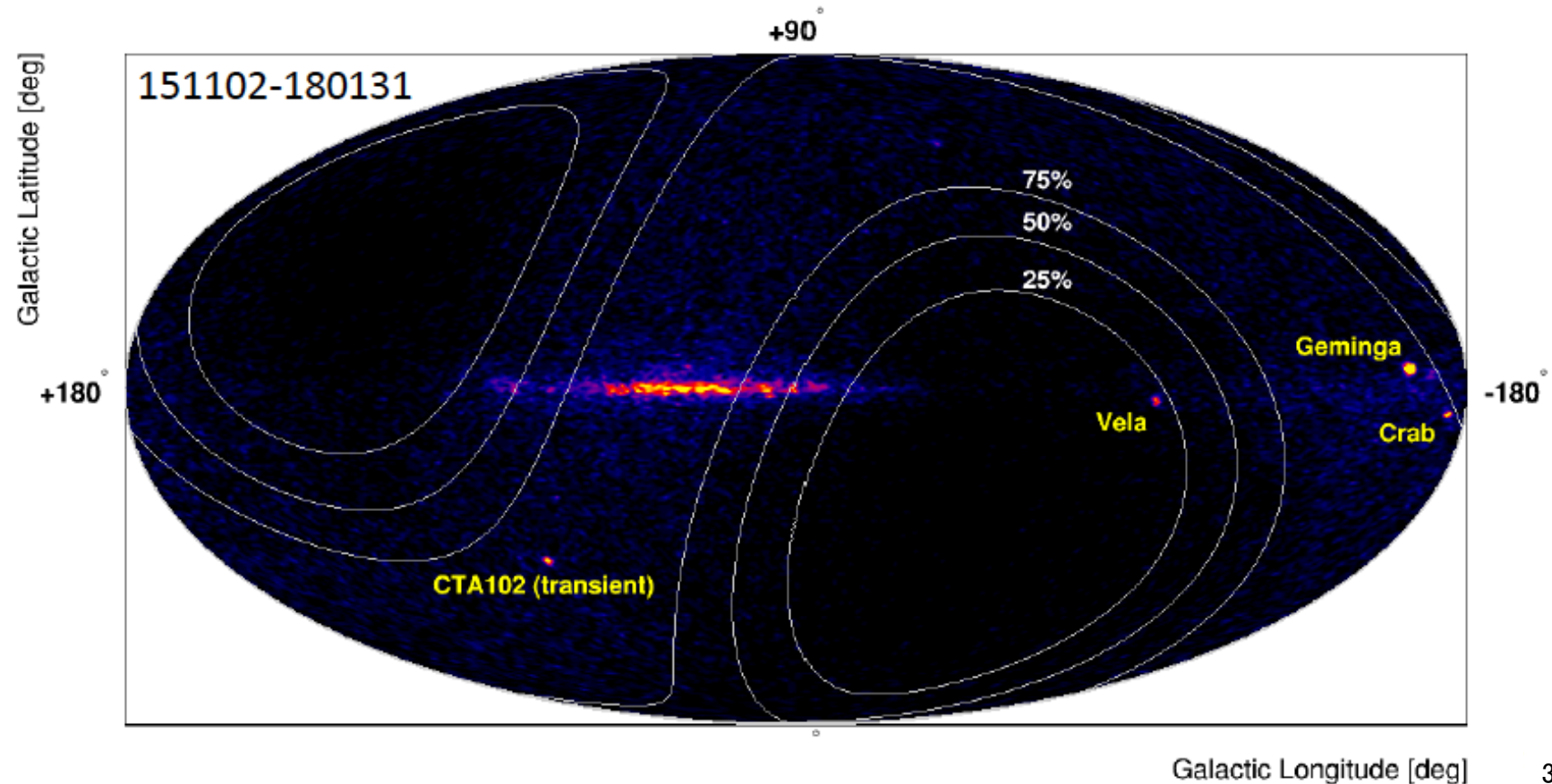
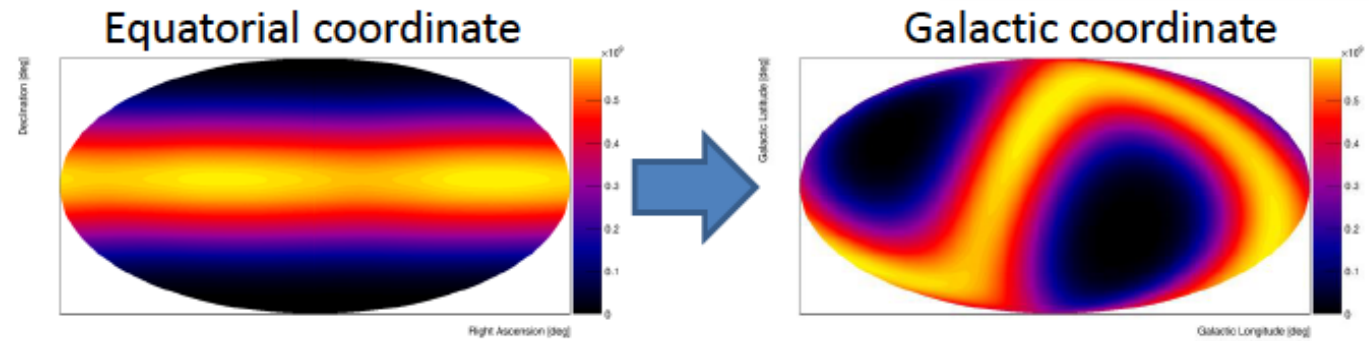


See also: E1.17-0022-18 (Mori & Asaoka)



CALET Sky Map w/ LE- γ Trigger ($E > 1\text{GeV}$)

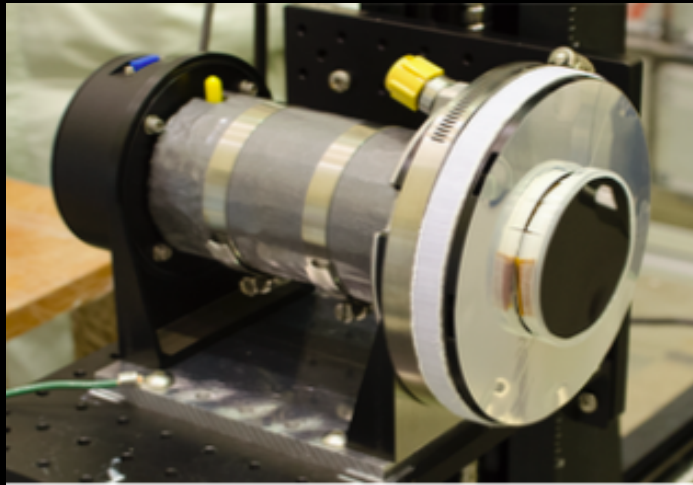
While exposure is not uniform, we have clearly identified the galactic plane and bright GeV sources.



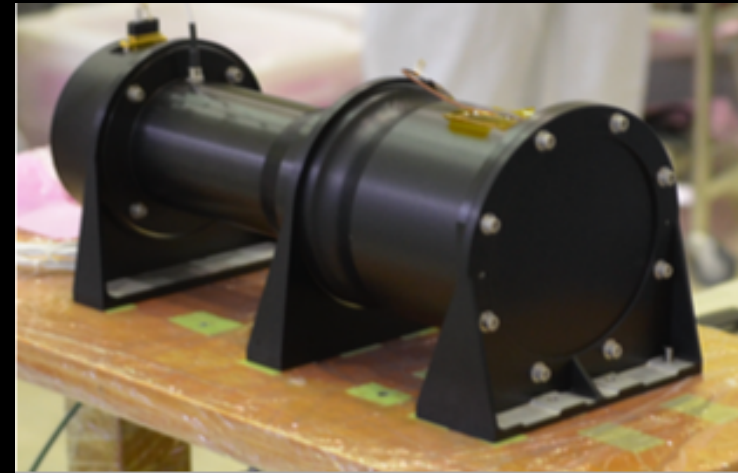


CALET Gamma-ray Burst Monitor (CGBM)

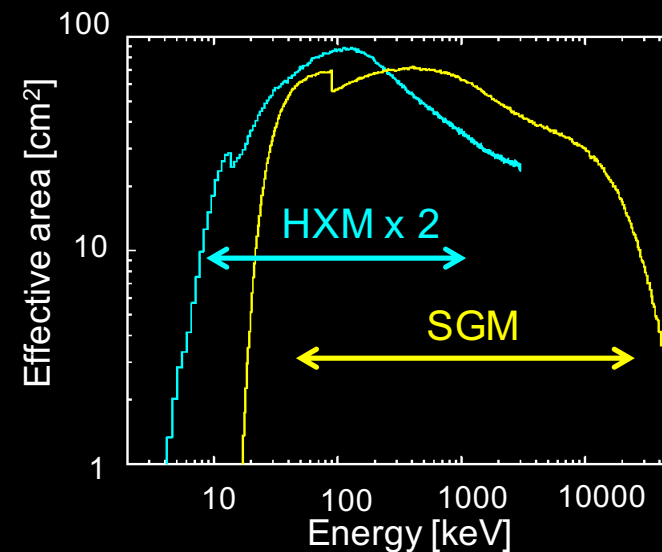
Hard X-ray Monitor (HXM)



Soft Gamma-ray Monitor (SGM)



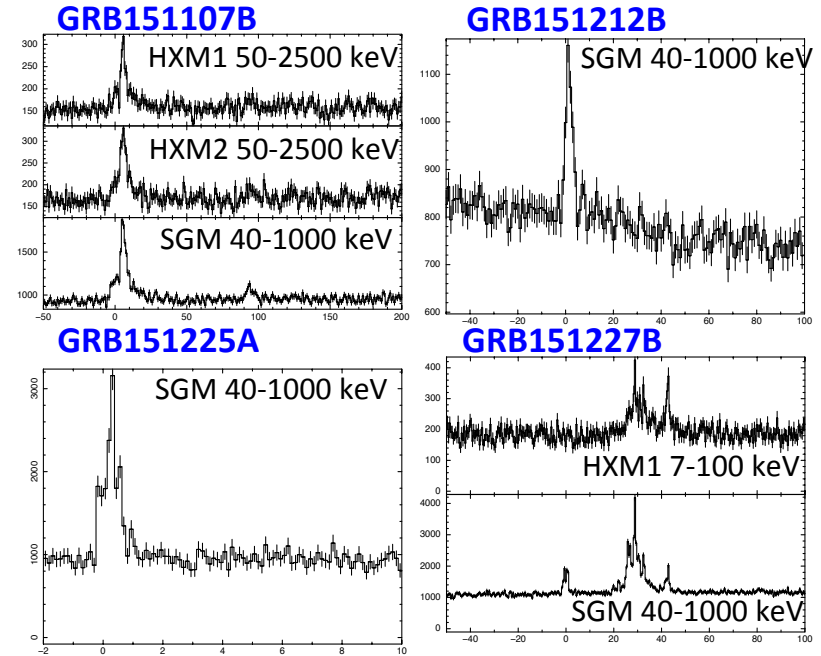
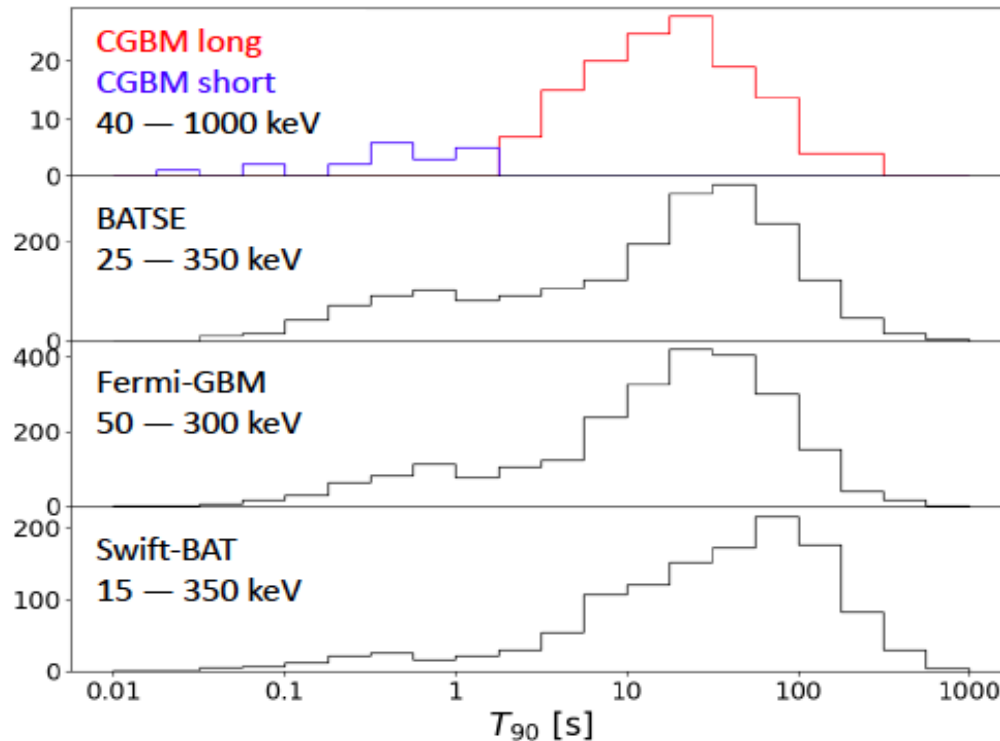
	HXM (x2)	SGM
Detector (Crystal)	LaBr ₃ (Ce)	BGO
Number of detectors	2	1
Diameter [mm]	61	102
Thickness [mm]	12.7	76
Energy range [keV]	7-1000	100-20000
Energy resolution@662 keV	~3%	~15%
Field of view	~3 sr	~2π sr



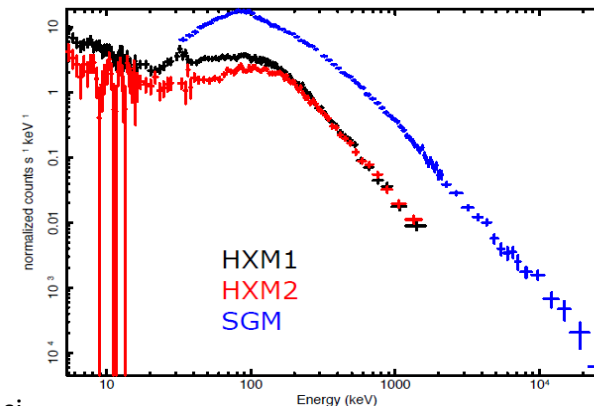


CGBM Observations Summary

Examples of Light Curves



Raw count spectra of GRB 160625B

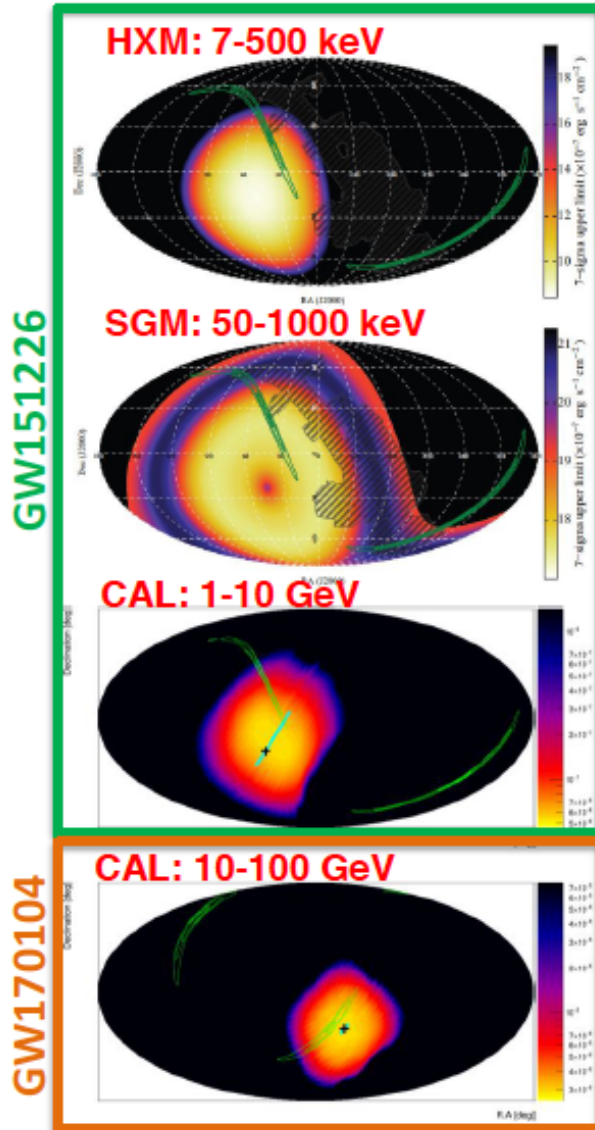


- ✧ As of June 2019:
- 159 GRBs detected
- 140 Long (88%) 19 Short (12%)
- Average rate ~ 43 GRBs/year



Complete Search Results for GW Events during O1&O2

GW151226: O. Adriani et al. (CALET Collaboration), ApJL 829:L20 (2016).
All O1 & O2: O. Adriani et al. (CALET Collaboration), ApJ 863 (2018) 160.



Event	Type	Mode	Sum. LIGO prob.	Obs. time	Upper limits	
					Ene. Flux erg cm ⁻² s ⁻¹	Lum. erg s ⁻¹
GW150914	BH-BH	Before operation				
GW151226	BH-BH	LE HXM SGM	15%	T ₀ -525 – T ₀ +211	9.3 x 10 ⁻⁸ 1.0 x 10 ⁻⁶ 1.8 x 10 ⁻⁶	2.3 x 10 ⁴⁸ 3-5 x 10 ⁴⁹
GW170104	BH-BH	HE	30%	T ₀ -60 – T ₀ +60	6.4 x 10 ⁻⁶	6.2 x 10 ⁵⁰
GW170608	BH-BH	HE	0%	T ₀ -60 – T ₀ +60	Out of FOV	
GW170814	BH-BH	HE	0%	T ₀ -60 – T ₀ +60	Out of FOV	
GW170817	NS-NS	HE	0%	T ₀ -60 – T ₀ +60	Out of FOV	

- CALET can search for EM counterparts to LIGO/Virgo triggers
- All O1 and O2 triggers checked – no signal in CGBM or CAL
- Upper limits set for GW151226 for CGBM+CAL in 2016 paper
- Upper limits for the CAL set using refined LE selection for triggers to-date in the 2018 paper



CALET: Summary and Future Prospects

- ❑ CALET was successfully launched on Aug. 19th, 2015. The observation campaign started on Oct. 13th, 2015. Excellent performance and remarkable stability of the instrument.
- ❑ As of May 31, 2019 total observation time is 1327 days with live time fraction to total time close to 84%. Nearly 1.8 billion events collected with low (> 1 GeV) + high energy (>10 GeV) triggers.
- ❑ Accurate calibrations have been performed with non-interacting p & He events + linearity in the energy measurements established up to 10^6 MIP.
- ❑ Measurement of **electron+positron spectrum** in 11 GeV - 4.8 TeV range using full acceptance
Observation of a flux reduction above 1 TeV.
- ❑ Direct measurement of **proton spectrum** in 50 GeV – 10 TeV energy range. Spectral hardening observed above a few hundred GeV.
- ❑ Preliminary analysis of primary elements up to Fe and secondary-to-primary ratios.
- ❑ Preliminary analysis of UH cosmic rays up to $Z=40$.
- ❑ Study of diffuse and point sources with gamma-rays. Follow-up observations of GW events in X-ray and gamma-ray bands. CALET's CGBM detected 159 GRBs in the energy range 7 keV-20 MeV.
- ❑ After an initial period of 2 years CALET observation time has been extended to 5 years at least.



CALET

Thank you
for your attention !



CALET Collaboration Team



O. Adriani²⁵, Y. Akaike², K. Asano⁷, Y. Asaoka^{9,31}, M.G. Bagliesi²⁹, E. Berti²⁵, G. Bigongiari²⁹,
W.R. Binns³², S. Bonechi²⁹, M. Bongio²⁵, P. Brogi²⁹, A. Bruno¹⁵, J.H. Buckley³², N. Cannady¹³,
G. Castellini²⁵, C. Checchia²⁶, M.L. Cherry¹³, G. Collazuol²⁶, V. Di Felice²⁸, K. Ebisawa⁸, H. Fuke⁸, T.G. Guzik¹³,
T. Hams³, N. Hasebe³¹, K. Hibino¹⁰, M. Ichimura⁴, K. Ioka³⁴, W. Ishizaki⁷, M.H. Israel³², K. Kasahara³¹,
J. Kataoka³¹, R. Kataoka¹⁷, Y. Katayose³³, C. Kato²³, Y. Kawakubo¹, N. Kawanaka³⁰, K. Kohri¹², H.S. Krawczynski³²,
J.F. Krizmanic², T. Lomtadze²⁷, P. Maestro²⁹, P.S. Marrocchesi²⁹, A.M. Messineo²⁷, J.W. Mitchell¹⁵, S. Miyake⁵,
A.A. Moiseev³, K. Mori^{9,31}, M. Mori²¹, N. Mori²⁵, H.M. Motz³¹, K. Munakata²³, H. Murakami³¹, S. Nakahira²⁰,
J. Nishimura⁸, G.A De Nolfo¹⁵, S. Okuno¹⁰, J.F. Ormes²⁵, S. Ozawa³¹, L. Pacini²⁵, F. Palma²⁸, V. Pal'shin¹,
P. Papini²⁵, A.V. Penacchioni²⁹, B.F. Rauch³², S.B. Ricciarini²⁵, K. Sakai³, T. Sakamoto¹,
M. Sasaki³, Y. Shimizu¹⁰, A. Shiomi¹⁸, R. Sparvoli²⁸, P. Spillantini²⁵, F. Stolzi²⁹, S. Sugita¹, J.E. Suh²⁹,
A. Sulaj²⁹, I. Takahashi¹¹, M. Takayanagi⁸, M. Takita⁷, T. Tamura¹⁰, N. Tateyama¹⁰, T. Terasawa⁷,
H. Tomida⁸, S. Torii^{9,31}, Y. Tunesada¹⁹, Y. Uchihori¹⁶, S. Ueno⁸, E. Vannuccini²⁵, J.P. Wefel¹³,
K. Yamaoka¹⁴, S. Yanagita⁶, A. Yoshida¹, and K. Yoshida²²

- 1) Aoyama Gakuin University, Japan
- 2) CRESST/NASA/GSFC and Universities Space Research Association, USA
- 3) CRESST/NASA/GSFC and University of Maryland, USA
- 4) Hirosaki University, Japan
- 5) Ibaraki National College of Technology, Japan
- 6) Ibaraki University, Japan
- 7) ICRR, University of Tokyo, Japan
- 8) ISAS/JAXA Japan
- 9) JAXA, Japan
- 10) Kanagawa University, Japan
- 11) Kavli IPMU, University of Tokyo, Japan
- 12) KEK, Japan
- 13) Louisiana State University, USA
- 14) Nagoya University, Japan
- 15) NASA/GSFC, USA
- 16) National Inst. of Radiological Sciences, Japan
- 17) National Institute of Polar Research, Japan

- 18) Nihon University, Japan
- 19) Osaka City University, Japan
- 20) RIKEN, Japan
- 21) Ritsumeikan University, Japan
- 22) Shibaura Institute of Technology, Japan
- 23) Shinshu University, Japan
- 24) University of Denver, USA
- 25) University of Florence, IFAC (CNR) and INFN, Italy
- 26) University of Padova and INFN, Italy
- 27) University of Pisa and INFN, Italy
- 28) University of Rome Tor Vergata and INFN, Italy
- 29) University of Siena and INFN, Italy
- 30) University of Tokyo, Japan
- 31) Waseda University, Japan
- 32) Washington University-St. Louis, USA
- 33) Yokohama National University, Japan
- 34) Yukawa Institute for Theoretical Physics, Kyoto University, Japan



CALET Collaboration Team



O. Adriani²⁵, Y. Akaike², K. Asano⁷, Y. Asaoka^{9,31}, M.G. Bagliesi²⁹, E. Berti²⁵, G. Bigongiari²⁹,
W.R. Binns³², S. Bonechi²⁹, M. Bongio²⁵, P. Brogi²⁹, A. Bruno¹⁵, J.H. Buckley³², N. Cannady¹³,
G. Castellini²⁵, C. Checchia²⁶, M.L. Cherry¹³, G. Collazuol²⁶, V. Di Felice²⁸, K. Ebisawa⁸, H. Fuke⁸, T.G. Guzik¹³,
T. Hams³, N. Hasebe³¹, K. Hibino¹⁰, M. Ichimura⁴, K. Ioka³⁴, W. Ishizaki⁷, M.H. Israel³², K. Kasahara³¹,
J. Kataoka³¹, R. Kataoka¹⁷, Y. Katayose³³, C. Kato²³, Y. Kawakubo¹, N. Kawanaka³⁰, K. Kohri¹², H.S. Krawczynski³²,
J.F. Krizmanic², T. Lomtadze²⁷, P. Maestro²⁹, P.S. Marrocchesi²⁹, A.M. Messineo²⁷, J.W. Mitchell¹⁵, S. Miyake⁵,
A.A. Moiseev³, K. Mori^{9,31}, M. Mori²¹, N. Mori²⁵, H.M. Motz³¹, K. Munakata²³, H. Murakami³¹, S. Nakahira²⁰,
J. Nishimura⁸, G.A De Nolfo¹⁵, S. Okuno¹⁰, J.F. Ormes²⁵, S. Ozawa³¹, L. Pacini²⁵, F. Palma²⁸, V. Pal'shin¹,
P. Papini²⁵, A.V. Penacchioni²⁹, B.F. Rauch³², S.B. Ricciarini²⁵, K. Sakai³, T. Sakamoto¹,
M. Sasaki³, Y. Shimizu¹⁰, A. Shiomi¹⁸, R. Sparvoli²⁸, P. Spillantini²⁵, F. Stolzj²⁹, S. Sugita¹, J.E. Suh²⁹,
A. Sulaj²⁹, I. Takahashi¹¹, M. Takayanagi⁸, M. Takita⁷, T. Tamura¹⁰, N. Tateyama¹⁰, T. Terasawa⁷,
H. Tomida⁸, S. Torii^{9,31}, Y. Tunesada¹⁹, Y. Uchihori¹⁶, S. Ueno⁸, E. Vannuccini²⁵, J.P. Wefel¹³,
K. Yamaoka¹⁴, S. Yanagita⁸, A. Yoshida¹, and K. Yoshida²²

